PHYSICAL THEORY OF PLASTICITY AND STRENGTH

V. L. INDENBOM and A. N. ORLOV

Usp. Fiz. Nauk 76, 557-591 (March, 1962)

DURING the 50 years elapsed since the discovery (in 1912) of diffraction of x rays by crystals and the development of the dynamic theory of the crystal lattice (1915), the physics of plasticity and strength has turned from a descriptive science with only formal premises into a major division of solid state physics, based on reliable experimental researches and on fully developed theoretical notions. The development of the physical theory of plastic deformation and failure is closely connected with the work of J. I. Frenkel, whose varied interests included basic problems in the theory of mechanical properties of both crystalline and non-crystalline solids. The present development of theoretical ideas and experimental methods of research on the real structure of solids has prepared the ground for the decisive stage in the development of the physics of plasticity and strength, namely the direct investigation of the atomic mechanism of plastic deformation and failure. This is most clearly pronounced in the case of crystalline bodies.

1. STRENGTH OF CRYSTALLINE BODIES AND STRENGTH OF INTERATOMIC BONDS

In 1926 Frenkel [1] showed that in the simplest model of a crystal atomic planes are ruptured or shifted whenever the elastic strains reach a critical value, on the order of several per cent. For example, for a simple cubic lattice the critical cleavage stress in the case of slipping of atomic planes is $\tau_0 = G/2\pi$ (G —shear modulus), while in the case of separating planes the critical stress is $\sigma_0 = 0.2\,E$ (E —Young's modulus). For a long time the values obtained for the rupture and shear strengths of crystals appeared to be unreasonably high and the discrepancy between the theoretical and real strength of crystals, amounting to several orders of magnitude, was discussed in the literature many times. Attempts at a more rigorous account of the lattice structure and of the character of interatomic bonds in the calculation of the theoretical strength did not result in appreciable changes in Frenkel's estimates. Thus, the value customarily assumed for the shear strength of a face-centered metal is usually that of MacKensie, [2] $\tau_0/G = 1/30$. The interatomic bonds are thus strong enough to withstand elastic strains of several per cent, and any premature failure should be ascribed to imperfections in the real crystals.

At the present time the full utilization of the interatomic bond strengths is no longer an unrealizable dream, for theoretical strength has been reached both in crystals practically free of imperfections (dislocations) and in defective crystals in which the dislocation mobility is suppressed. Characteristic examples are given in Table I.

In silicon crystals without dislocations or with immobile dislocations, the theoretical strength of the interatomic bonds is realized almost completely, but here, too, the maximum elastic strain obtained in experiment apparently corresponds to the creation of new dislocations not in the ideal lattice, but on chemical inhomogeneities or surface defects. In filamentary crystals (whiskers) the dislocations lie as a rule along the axis, thus preventing the multiplication of dislocations, needed to produce noticeable plastic deformation. Filamentary crystals with nearly theoretical strength have been obtained by now for a great variety of materials with different types of interatomic bonds and crystal structures (metals with face-centered and body-centered cubic, hexagonal, and other lattices, oxides such as ZnO or Al_2O_3, alkali-halide compounds, nitrides, carbides, graphite, organic crystals, and others). [3,4] Hexagonal metals have high tensile strength in a direction perpendicular (and parallel) to the base because the effective cleavage stresses, which cause the motion of the dislocations in the glide planes, are reduced in this crystal orientation. The ultimate strength coincides here practically with the yield point, which occurs when critical cleavage stress is reached for the most favorable glide system. In materials with finely dispersed structure such as hot worked steel, the dislocations, the interphase boundaries, and other imperfections are very dense. This makes plastic deformation so difficult that the strength of the material approaches the strength of the interatomic bonds. For comparison we also list in Table I data on the strength of quartz filaments and fused quartz, whose high strength is apparently due to the elimination of the most dangerous surface defects, just as in the Ioffe effect.

Roughly speaking, the strength of a solid approaches the theoretical value in two limiting cases —in bodies without defects and in bodies greatly spoiled by defects. In all other cases the macroscopic strength is lower than theoretical (frequently by two or three orders of magnitude). Naturally, the theoretical strength is attained in this case, too, but only in highly localized fashion, in the overstressed portions. Therefore the process of deformation and failure of solids cannot be understood without a specific analysis of the real structure of the body and its variation during the loading process.

Table I. Shear and rupture strength of certain materials

Source	Material	$\tau/G(\%)$	$\sigma/E(\%)$
1	Dislocation-free Si crystals at 900°C	0.12	–
2	Si crystals at room temperature	>2	>2
3	Defect-free portions of LiF crystals	1.2	–
4	NaCl crystals in water (Ioffe effect)	–	3.6
5	Filamentary crystals of Si	–	3.6
6	Filamentary crystals of Fe	6	4.9
	Filamentary crystals of Cu	2.2	2.8
	Filamentary crystals of Ag	3.3	4
7	Filamentary crystals of NaCl	3	2.6
8	Zn crystals; tension perpendicular to base	—	0.1–5
9	Be crystals; compression perpendicular to base	0.7	–
10	Sb wire (30 μ diameter)	–	0.25
11	Steel after hot working	1.6	1.2
12	Quartz filaments	–	10–25
13	Fused quartz	–	19

1. W. C. Dash, Bull. Amer. Phys. Soc. 4, 47 (Abstr. Ser. A11) (1959).
2. Pearson, Read, and Feldman, Acta Metallurgica 5, 181 (1957); W. C. Dash, Growth and Perfection of Crystals, Wiley, N. Y., 1958, p. 189.
3. J. Gilman, J. Appl. Phys. 30, 1584 (1959).
4. Ioffe, Kirpicheva, and Levitskaya, Z. Physik 22, 286 (1924).
5. C. C. Evans, cited by J. E. Gordon in "Growth and Perfection of Crystals," 1958, p. 218.
6. S. S. Brenner, Growth and Perfection of Crystals, 1958, p. 157.
7. Z. Gyulai, Z. Physik 138, 317 (1954).
8. M. V. Klassen-Neklyudova, Techn. Phys. USSR 5, 827 (1938); J. J. Gilman, Trans. AIME 212, 783 (1958).
9. Garber, Gindin, and Shubin, FTT 3, 918 (1961), Soviet Phys. Solid State 3, 667 (1961).
10. G. F. Taylor, Phys. Rev. 23, 655 (1924).
11. F. G. MacGuire, Missiles and Rockets, Sept. 28 (1959); see also review: M. G. Lozinskiĭ, Vestnik mashinostreniya (Machinebuilding bulletin) No. 1, 56 (1961).
12. S. M. Zhurkin, Phys. Z. Sowjetunion 1, 123 (1932); Techn. Phys. USSR 1, 386 (1935); F. O. Anderegg, Ind. Eng. Chem. 31, 290 (1939).
13. W. B. Hillig, J. Appl. Phys. 32, 741 (1961).

2. IMPERFECTIONS IN CRYSTALS

Until recently the discrepancy between theoretical and experimental data on strength and other structure-sensitive properties of crystals were meaninglessly "explained" as being due to the imperfections in the real structure of the crystal. Yet is was J. I. Frenkel who started to construct the physical theory of lattice imperfections, which by now has become an important independent branch of solid state physics and has found brilliant experimental confirmation. Frenkel first introduced the notion of vacancies ("holes") and interstitial atoms in a crystal lattice. He also studied quantitatively, together with T. A. Kontorova, the atomic model of the edge ("transverse") and screw ("longitudinal") dislocations, introduced the notion of twin ("orientational") dislocation, etc.

From the purely geometrical point of view, lattice defects can be classified by the number of directions in which the inelastically distorted region has macroscopic dimensions, with dimensions in the remaining directions that are microscopic, on the order of several interatomic distances (Fig. 1). The vacant sites, the interstitial atoms, and the impurity atoms are zero-dimensional (point) defects, dislocations and chains of point defects are one-dimensional (linear defects), and boundaries between crystallites and mosaic blocks, stacking faults, and twin boundaries are two-dimensional (surface) imperfections. The natural unit for measuring the energy of defects is the quantity Gb^3 for point imperfections, Gb^2 for linear imperfections, and Gb for surface imperfections, where G is the shear modulus and b is the minimum parameter of the lattice translation. For

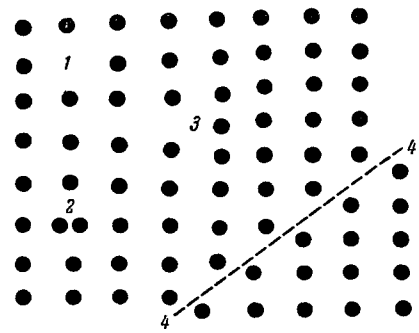

FIG. 1. Various defects in fcc lattice. 1 – Vacancy; 2 – interstitial atom; 3 – edge dislocation; 4 – stacking fault. The plane of the figure corresponds to the (110) plane, and the [001] direction is horizontal.

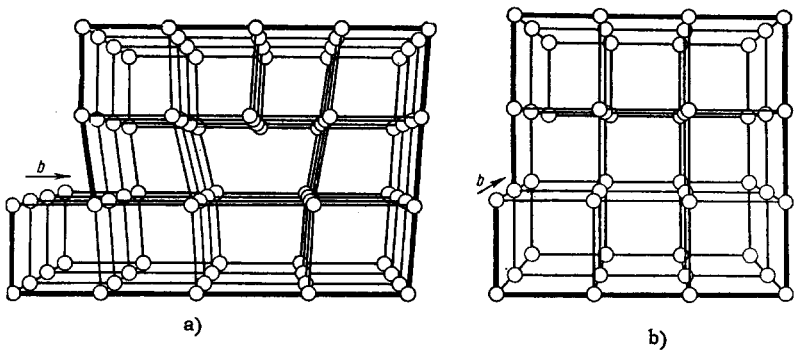

FIG. 2. Dislocation in simple cubic lattice. a) Edge dislocation; b) screw dislocation. The Burgers contour is shown by the heavier line, and the Burgers vector is indicated by the arrow.

example, the energy of vacancies is about 0.2 Gb^3, the energy of dislocations (per unit length) is usually estimated at 0.5 Gb^2, while the surface energy of the crystal is on the order of 0.1 Gb.

Point defects. In addition to the isolated vacancies and interstitial atoms investigated by Frenkel,[5] modern theory considers more complicated point defects; in particular, bivacancies in cubic face-centered and diamond lattices turn out to be more mobile than single vacancies. Electric effects observed in the deformation of ionic crystals, are connected with the presence of oppositely charged vacancies and interstitial ions. The interaction between point defects and electrons leads to the appearance of various color centers.

Experimental data as well as model calculations (especially with electronic computers) have made it possible to determine more precisely the distribution of atoms near point defects and to explain some of the experimentally observed facts. It turns out, for example, that in f.c.c. lattices interstitial atoms are located not in the centers of the edges, but displace one of the lattice atoms from its site, forming with it a pair ("dumbbell") oriented along the axis of the cube with the center of gravity in the site (see Fig. 1).[6,7] The height of the barrier that prevents recombination of the Frenkel pair (vacancy–interstitial atom) depends sharply on the orientation, since spontaneous annihilation of a pair occurs if the distance between the partners is less than two interatomic distances for pairs oriented along [100] and less than four distances for pairs along [110]. Recently point defects were observed in an ion projector.[8] Accumulations of point defects are observed in an electron transmission microscope.

Line defects. The most important role in plastic deformation and rupture is played by the dislocations. Geometrically, a dislocation is completely defined by the Burgers vector **b**, which is equal to the circulation of the displacement vector **u** along an arbitrary contour L enclosing the dislocation:

$$b_i = -\oint_L \frac{\partial u_i}{\partial x_j}\, dx_j. \qquad (2.1)$$

If a circuit were made up of translation vectors so that it would be closed in an ideal lattice, then this circuit (Burgers circuit) would remain open if constructed along the dislocation line, and the non-closure is equal to the Burgers vector (Fig. 2). Consequently the Burgers vector of a dislocation in a crystal is equal to the lattice translation vector.

The angle ψ between the dislocation line and the Burgers vector defines the orientation of the dislocation. If $\psi = 90°$, the dislocation is called an edge dislocation* and is the edge of the incomplete atomic plane that is made discontinuous inside the crystal (Fig. 2a). If $\psi = 0$, the dislocation is called a screw dislocation (Fig. 2b), the crystal actually consisting of a single atomic plane bent along a helical surface. The dislocation is the axis of the helix and the Burgers vector is equal to the pitch of the screw.

For other values of ψ, dislocations of mixed orientations are obtained (Fig. 3). In the general case the dislocation line is an arbitrary curve in space, along which the Burgers vector remains constant (although the orientation of the dislocation may vary). In Fig. 3 the orientation of the dislocation goes over gradually from that of an edge dislocation (through the mixed state) into that of a screw dislocation. Like vortex lines in hydrodynamics, the dislocation lines cannot be discontinuous inside the body and must either close on themselves (dislocation loops), emerge from the free surface, or else branch into other dislocations. In the latter case a theorem analogous to Kirchhoff's law for currents applies: if all the dislocations are regarded as moving towards the node, the sum of the Burgers vectors should be equal to zero.

As can be seen from Fig. 3, the dislocation is the boundary between the region of the glide plane along which a displacement equal to the Burgers vector took place. If the direction of the shear is perpendicular to the boundary of the region, the dislocation has an edge orientation, if it is parallel, it has a screw orientation.

The elastic strains and stresses around the dislocations are proportional to the Burgers vector, while the dislocation energy is proportional to the square of the Burgers vector, and consequently two dislocations repel each other if their Burgers vectors make an acute angle, and attract each other if this angle is obtuse.

*In some translations an edge dislocation is inappropriately called a "line" dislocation, although any dislocation is a line defect.

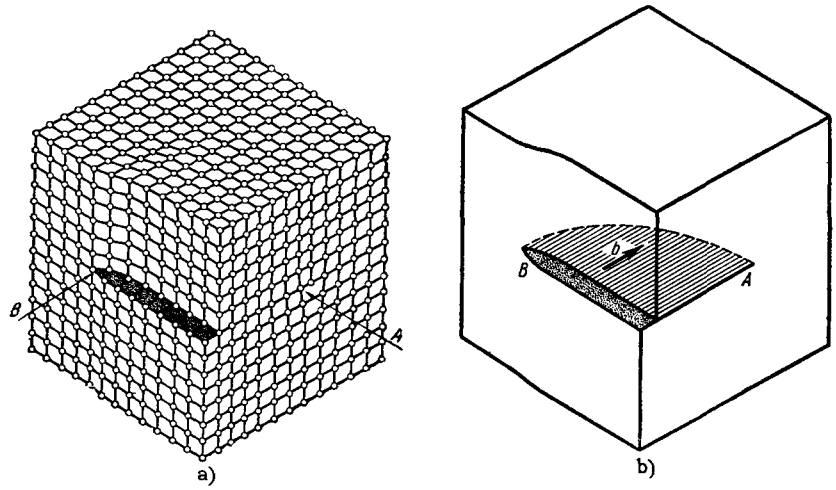

FIG. 3. Curvilinear dislocation which changes its orientation from edge type (A) (through mixed type) to a screw dislocation (B). a) Atomic arrangement; b) dislocation as boundary of section of local slip region (part of the glide plane is shown shaded). The Burgers vector is designated by the arrow.

As a result of this attraction, the dislocations may coalesce (dislocation reaction).

Various direct methods have been developed for the observation of dislocations in crystals:[9] selective etching, decoration, x-ray microphotography, transmission electron microscopy (directly or by the moire pattern), investigation of the topography of the crystal surface in an optical or electron microscope and in electron and ion projectors, and observation of stresses around the dislocation by the photoelasticity method.

Surface defects. The surface defects most frequently encountered in crystals, namely the block boundaries, are actually arrays and networks of dislocations. The simplest examples are shown in Fig. 4. A family of parallel edge dislocations (Fig. 4a) forms a small-angle boundary of blocks turned through an angle $\theta = b/h$ relative to each other about an axis parallel to the dislocations, (b is the Burgers vector and h is the distance between dislocations). This relation was verified many times in different crystals.

If the block-rotation axis does not lie in the plane of the boundary, then the block separation surface should be made up of at least two intersecting dislocation families (Fig. 4b). The quadruple nodes in the dislocation networks are usually not favored from the energy point of view and break up into pairs of triple junctions in accordance with the scheme of Fig. 4c. The result is a hexagonal network of the type of Fig. 4d.

As the block disorientation angle increases, the dislocations forming the boundaries come closer together and when the disorientation is on the order of 15—20° they lose their individuality. A large-angle boundary is formed, namely a surface defect which does not consist of line defects. The atomic structure of such boundaries is under study at the present time.*

*Extensive large-angle boundaries can be made up in individual cases of three-dimensional (but not planar) networks of dislocations.[10]

Other types of surface defects which cannot be reduced to an aggregate of line defects are the twin boundaries and stacking faults. A stacking fault is essentially a twin layer one atom (see Fig. 1) or two atoms thick. In single-atom lattices with closest spherical packing (fcc and hexagonal) the stacking faults are produced in $\{111\}$ planes in which the correct sequence of the atomic layers is violated (for example ABCBCABC in Fig. 1).

Partial dislocations. The ordinary (perfect) dislocations considered above, with a Burgers vector equal to the lattice translation vector, are not boundaries of a two-dimensional imperfection. A different type of linear imperfection is formed by boundaries of stacking faults, which is discontinuous inside the crystal (partial dislocations) (Fig. 5a), and jogs on twin boundaries (twinning dislocations) (Fig. 5b). The Burgers contour for a partial dislocation is constructed in such a way as to make the contour closed not in an ideal crystal, but in a crystal with a through stacking fault. In similar fashion, for a twinning dislocation, the Burgers contour should be closed in a crystal with plane (coherent) twin boundary. When so defined, the Burgers vector of partial and twinning dislocations is smaller than the lattice translation vector.

Perfect dislocations that lie in closely packed planes can dissociate into partial dislocation with formation of a stacking-fault strip between them. In fcc crystals (Fig. 5c) the dissociation is in accordance with the reaction

$$\frac{1}{2}[110] = \frac{1}{6}[211] + \frac{1}{6}[12\bar{1}].$$

The partial dislocations A and B repel each other with a force (per unit length) $F \approx Gb^2/2\pi r$, which is counteracted by the surface tension γ_0 of the stacking fault. As a result, the equilibrium width of the split dislocation is $\sim Gb^2/2\pi\gamma_0$. In aluminum ($\gamma_0 = 200$ erg/cm^2) the dislocations practically do not dissoci-

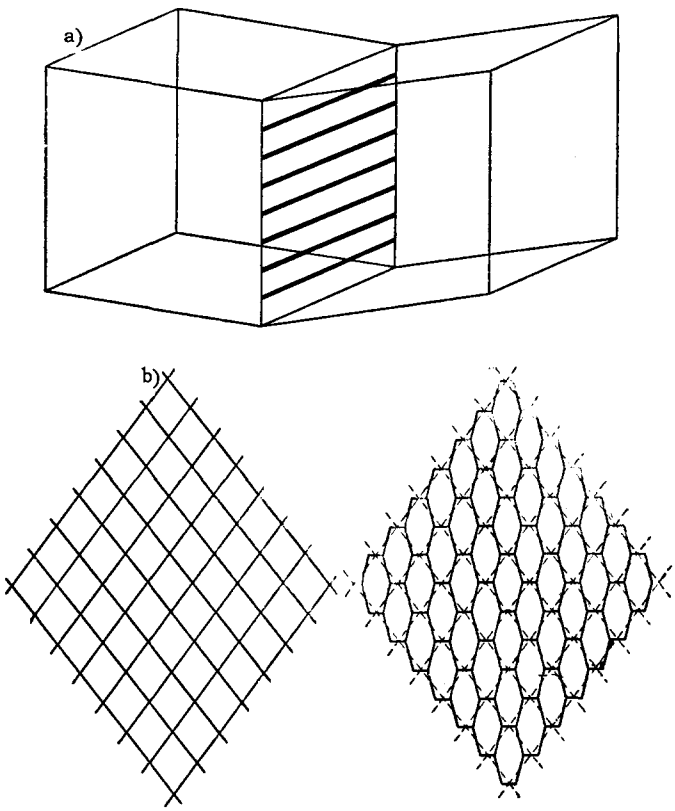

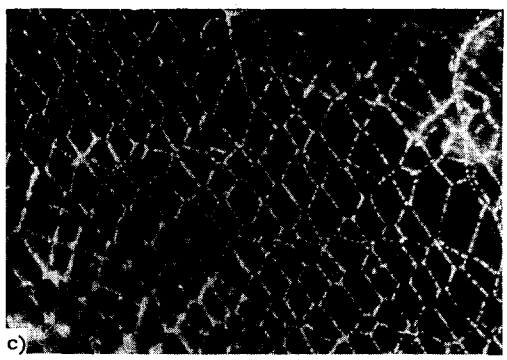

FIG. 4. Dislocation structure of block boundaries. a) Vertical wall of dislocations (inclination boundary), characteristic of polygonization and fault blocks; b) example of boundary made up of a network of dislocation; c) more stable network, made up of network (b) by splitting the quadruple nodes into triple ones; d) dislocation grid in KCl, disclosed by the decoration method (Dekeyser and Amelinckx).[9]

ate while in copper ($\gamma_0 = 40$ erg/cm^2) the width of the strip is equal to 8b.*

The dissociation of the dislocation is clearly observed in a transmission electron microscope in many face-centered metals, graphite, talcum, and other materials. Twinning dislocations can be observed not only by transmission in an electron microscope, but also by the method of selective etching.

*We note that different experimental methods yield for γ_0 results which do not always coincide.

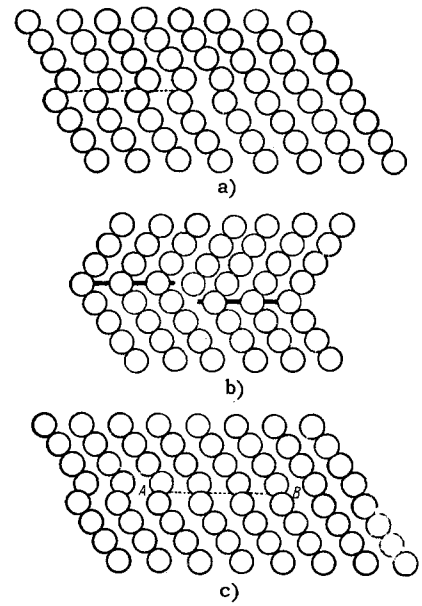

FIG. 5. Partial dislocations in fcc lattice. The plane of the figure is (110), and the [1$\bar{1}$2] direction is horizontal. a) Partial Shockley dislocation (stacking fault denoted by dashed line); b) twinning dislocation (jog on the twin boundary); c) split edge dislocation, consisting of partial dislocations A and B and a stacking fault strip AB between them.

3. PLASTIC DEFORMATION AS MOTION OF DEFECTS

Irreversible displacement of lattice defects (and only this type of displacement) causes irreversible changes in the form of the crystal (plastic deformation). In evaluating the role of the displacement of different structural defects, J. I. Frenkel emphasized the difference between diffusion flow, caused by motion of point defects and plastic flow, caused by the motion of the dislocations.

Under the influence of a stress σ in a body with linear dimensions on the order of L, the motion of point defects (for the most part, vacancies) results in a rate of plastic deformation[12]

$$\dot{e} = \frac{D}{L^2}\frac{\sigma\Omega_0}{kT}, \qquad (3.1)$$

where D is the self-diffusion coefficient, Ω_0 —atomic volume, $L = \sqrt{3}\,R/2$ for a spherical grain with radius R. Diffusion plasticity plays a major role in the creep of fine-grain materials at high temperatures. In all other cases, as a rule, the main contribution to plastic deformation is made by motion not of point defects, but of dislocations.

The mechanisms of displacement of dislocations in the glide plane (plane passing through the dislocation line and the Burgers vector) and perpendicular to it are different. In the former case (glide) the atoms are displaced only through small distances (smaller than the lattice parameter), while in the second case (climb) the incomplete atomic planes are either in-

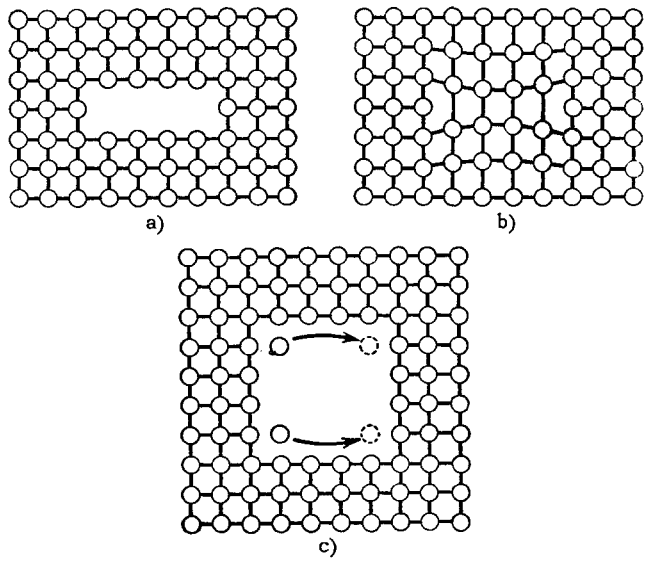

FIG. 6. Formation and conservative climbing of prismatic dislocation. a) Planar accumulation of vacancies (section through the accumulation axis); b) collapse of the accumulation a produces a dislocation ring (prismatic dislocation); c) migration of the atoms along the dislocation leads to climbing of the ring as a whole (section through the plane of the ring).

creased or shortened, and this calls for mass transfer —a diffusion of the vacancies or of the interstitial atoms. In both cases the speed of plastic deformation is given by a formula such as (see Sec. 4 for more details)

$$\dot{e} = Nvb, \tag{3.2}$$

where N is the density of the dislocations and v their velocity. The dislocations may glide with velocities up to that of sound, as first predicted by Frenkel and Kontorova. If the density of the mobile dislocations is N $= 10^8$ cm^{-2}, the limiting velocity of plastic deformation accompanying the glide of the dislocation reaches 10^5 sec^{-1}. If it is recognized that the force acting per unit dislocation length in the field of stress σ is equal to $F = b\sigma$, the rate of the climb of the dislocation, limited by self diffusion, is

$$v = \frac{2\pi D}{b \ln (R/r_0)} \frac{\sigma \Omega_0}{kT}, \tag{3.3}$$

where R is the radius of the grain and r_0 is the radius of the dislocation core, which captures or emits point defects. From (3.2) and (3.3) we obtain for the rate of plastic deformation accompanying the climb of the dislocations

$$\dot{e} = \frac{2\pi ND}{\ln (R/r_0)} \frac{\sigma \Omega_0}{kT}. \tag{3.4}$$

Comparison of (3.1) and (3.4) shows that the contribution from climb exceeds the contribution from diffusion plasticity by a factor $3\pi NR^2/2 \ln (R/r_0)$, i.e., by several orders of magnitude. Even when $r_0 \sim b$ and $R \sim (10^3 - 10^4)b$, a climb of five or six dislocations guarantees the same rate of plastic deformation as the diffusion flow of all the point defects alone.

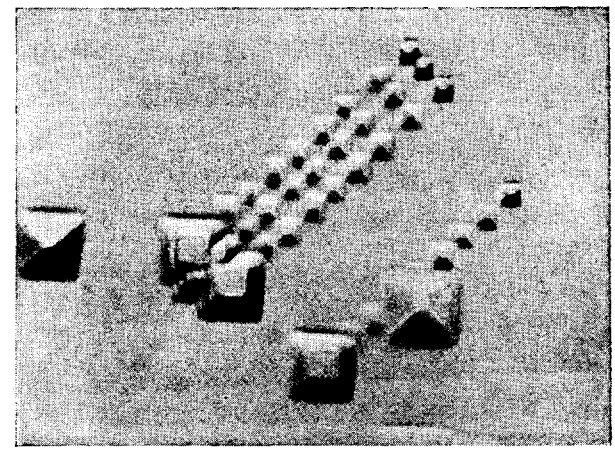

FIG. 7. Jump-like motion of dislocations in NaCl. Method of continuous selective etching.[13]

When gliding dislocations cross, jogs which do not lie in the glide plane form on the dislocations. Further gliding of the dislocations forces the jogs to climb and to leave a trail of chains of vacancies or interstitial atoms. Consequently, a large number of point defects are produced during the course of plastic deformation and change the density, electric resistivity, the diffusion coefficient, and other properties of the crystal.

An anomalously high rate of climb is observed for dislocation loops that result from a collapse of flat accumulations of vacancies (Fig. 6). The point defects migrate in this case not over the volume of the crystal, but along the dislocations, causing the growth of an incomplete atomic plane on one side of the loop, due to the atoms that are released during the climb over the opposite side of the loop.

Partial dislocations move as a rule by slipping (the stacking faults prevent climbing). Consequently, partial dislocations with a Burgers vector that does not lie in the plane of the stacking fault are practically immobile (sitting dislocations). A tangential displacement (slip) of twinning dislocations along the boundary of the twin causes a normal displacement of this boundary.

Simultaneous motion of dislocations making up a block boundary also leads to plastic deformation. For a crystal made of blocks with dimension L, with average disorientation angle θ, the rate of deformation is

$$\dot{e} = \frac{v\theta}{L}, \tag{3.5}$$

where v is the speed of the boundary. Formula (3.5) coincides, of course, with formula (3.2).

The motion of dislocations is observed most effectively either directly in a transmission electron microscope or by the selective etching method. Repeated etching fixes the initial and final positions of the dislocations, while continuous etching during the time of deformation makes it possible to follow the kinetics of the dislocation displacement (Fig. 7). The most complete information is obtained using electron micro-

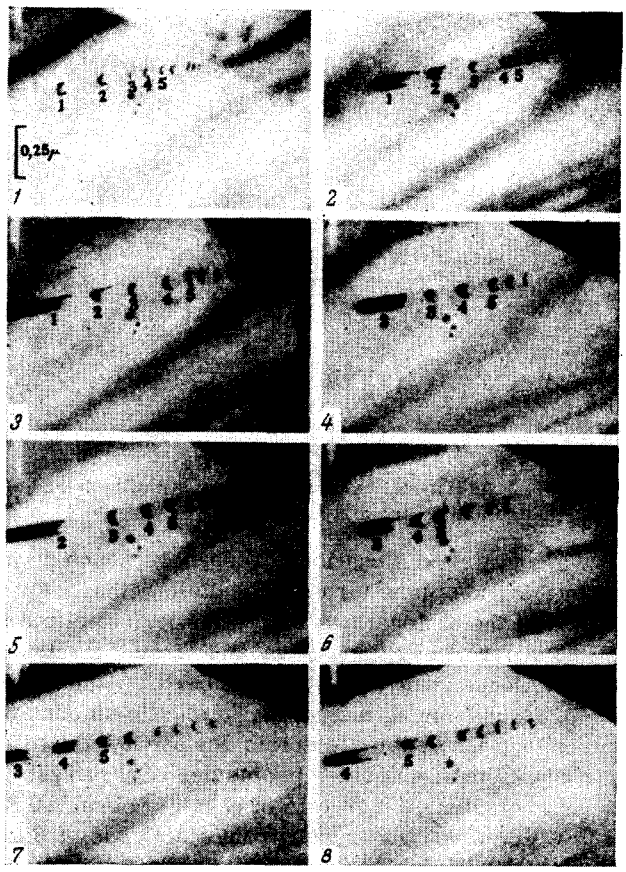

FIG. 8. Motion of dislocations in stainless steel. Motion picture frames taken in a transmission electron microscope. The first five dislocations are numbered.[14]

scopes equipped with an attachment for deforming the specimen under the beam and with a motion picture camera. An example of pictures that illustrate the motion of dislocations in stainless steel is shown in Fig. 8.

4. MATHEMATICAL FORMALISM OF DISLOCATION THEORY

In the preceding sections we used, in simplified form, certain formulas of dislocation theory. At the present time the formalism of the theory has been rather fully developed, and many plastic deformation phenomena can be rigorously described.[15-20]

Dislocations in elasticity theory. Long after they were experimentally observed in crystals, dislocations were regarded in the mathematical theory of elasticity as linear elastic-field singularities characterized by condition (2.1) or by even more general conditions.[21] Dislocation theory is now as inseparable a part of elasticity theory as is the theory of vortices in hydrodynamics or the theory of currents in electrodynamics.

In a cylindrical coordinate system (r, φ, z) the stresses around a straight edge dislocation in an unbounded isotropic medium with a Poisson coefficient ν are given by

$$\sigma_{rr}=\sigma_{\varphi\varphi}=\frac{\sigma_{zz}}{2\nu}=-\frac{Gb}{2\pi(1-\nu)}\frac{\sin\varphi}{r},\quad \sigma_{r\varphi}=\frac{Gb}{2\pi(1-\nu)}\frac{\cos\varphi}{r} \tag{4.1}$$

(the azimuth φ is measured from the direction of the Burgers vector); for a screw dislocation

$$\sigma_{z\varphi}=\frac{G}{2\pi}\frac{b}{r}. \tag{4.2}$$

The elastic field of an arbitrary dislocation can be written in the form of a contour integral. In particular, for displacements around a dislocation circuit characterized by a Burgers vector **b**, i.e., characterized by condition (2.1), the following Burgers formula holds true

$$\mathbf{u}(\mathbf{r})=\frac{\mathbf{b}\Omega}{4\pi}+\frac{\mathbf{b}}{4\pi}\times\oint_L\frac{d\mathbf{r}'}{R}+\operatorname{grad}\frac{\mathbf{b}}{8\pi(1-\nu)}\oint_L\mathbf{R}\times\frac{d\mathbf{r}'}{R}, \tag{4.3}$$

where Ω is the solid angle subtended by the contour L from the point **r**, and $\mathbf{R}=\mathbf{r}-\mathbf{r}'$. It was recently shown [23] that in the general case, including that of a bounded body and an isotropic medium, the influence functions for the dislocations coincide with the stress functions Φ (σ = curl Φ) for a concentrated force. In particular, we can use in place of the Burgers formula

$$u_i=b_j\oint_L dL_k\Phi_{kj}^{(i)}. \tag{4.4}$$

The elastic dislocation field can also be constructed from a stress function χ (σ = curl (curl χ)*),[16]

$$\chi_{ij}-\frac{\nu}{\nu+2}\chi_{kk}\delta_{ij}=\frac{G}{8\pi}\Big(e_{ikl}b_l\nabla_k\oint_L|r-r'|\,dx_j'$$
$$\text{symmetrical term}\Big), \tag{4.5}$$

where e_{ijk} is the unit antisymmetrical tensor.

The energy of interaction between a dislocation and an arbitrary field of stresses σ can be expressed also in the form of a contour integral. Variation yields for the configuration force dF acting on an element dL of the dislocation line the expression

$$dF_j=e_{ijk}\,dL_j\sigma_{kl}b_l. \tag{4.6}$$

The interaction energy of two dislocations can be accordingly written down in the form of a double contour integral.[24]

Rigorous solutions have been found for the simplest cases of moving dislocations.[25-27] In addition to the static force (4.6), a dislocation displaced in a moving medium also experiences a "Lorentz" force proportional to the speed of the dislocation and to the speed of the medium.[27]

The theoretical stress field around the dislocations in crystals can be checked not only indirectly (from the configuration of the dislocation lines), but also directly by the photoelasticity method. Figure 9a shows a photograph of the stresses around edge and mixed dislocations in a silicon plate, obtained by the method of [28]. The stress rosettes are in good agreement with (4.1).

Calculation of the stresses due to the dislocations

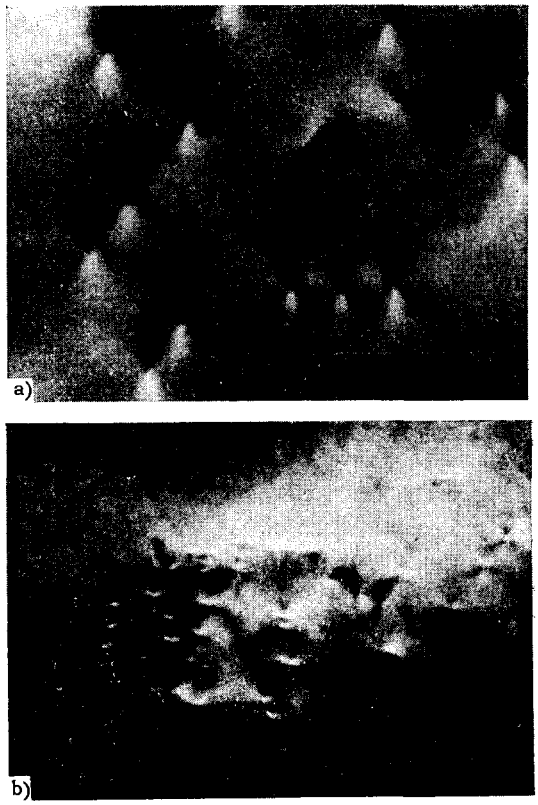

FIG. 9. Internal stresses due to dislocations in silicon. Polarization inframicroscope. a) Stresses around the dislocations; the long lobes of the birefringence rosettes lie along the Burgers vector; b) macro- and microstresses.

permits a new treatment of the theory of internal stresses, since it is precisely the dislocations that serve as a rule as main source of internal stresses in crystals. This raises anew the question of classification of internal stresses. Each dislocation yields in principle a field that decreases slowly (as 1/r). The fields of the neighboring dislocations, becoming superimposed, can either produce long-range macroscopic stresses, or can cancel each other out at distances on the order of the distance between dislocations (microstresses). Figure 9b shows examples of both macrostresses (horizontal row of dislocations in the upper part of the figure) and microstresses (vertical row of dislocations on the left). It is apparently necessary to review the present x-ray diffraction treatment of internal stresses, and re-base it on a theoretical pattern of x-ray scattering by crystals with different dislocation configurations.[29]

Macroscopic description of dislocations. For bodies with a large number of dislocations it is advantageous to introduce for the dislocations a distribution function $f_{\mathbf{b}}(\mathbf{n}, \mathbf{r})$, where $df = f_{\mathbf{b}}\, dV\, d\Omega$ is the summary length of the dislocations with Burgers vector **b**, passing near the point **r** through the volume dV and located within the solid angle $d\Omega$ about the direction **n**. The summary density of the dislocations (the summary length of dislocation lines per unit volume)

$$N = \int (d\mathbf{b}) \int d\Omega\, f_{\mathbf{b}} \tag{4.7}$$

determines in first approximation the latent energy, the increase in the volume, the additional electric resistivity, and other effects.

Macroscopic stresses and lattice rotations are defined by means of the so-called macroscopic dislocation density tensor β_{ij}, the ij-th component of which is equal to the j-th component of the summary Burgers vector of all the dislocations crossing a unit area perpendicular to the i axis.[16] It is obvious that

$$\beta_{ij} = \int (d\mathbf{b}) \int d\Omega\, n_i b_j f_{\mathbf{b}}. \tag{4.8}$$

In (4.7) and (4.8) it is necessary to take into account in the integration only the positive directions of the vector **b** (to integrate over a hemisphere). In crystals, the Burgers vectors run through a discrete set of values (in practice it is sufficient to take into account only several values), and the integrals with respect to **b** are replaced by sums. As a result, the tensor β_{ij} is made up of dyads of the type $P_i b_j$, which describe the flux **P** of dislocations with Burgers vector **b**.[30] If the mixed dislocations are arbitrarily broken up into parts with pure edge orientation and parts with pure screw orientation, the longitudinal component of **P** (along the Burgers vector) will describe the density of the screw dislocations, and the transverse component (perpendicular to **b**) will describe the density of the edge dislocations. In particular, in a simple cubic lattice, in which the Burgers vectors are directed along coordinate axes aligned with the axes of the cube, the diagonal terms of β_{ij} describe the density of the screw dislocations, and the non-diagonal terms the density of the edge dislocations.[31]

While the Burgers vector **b** is defined in accordance with (2.1) as the circulation of the displacement vector, the tensor β corresponds in analogous fashion to the circulation of the elastic distortion ϵ, comprising the symmetrical elastic deformation tensor e and the antisymmetrical lattice rotation tensor ω, equivalent to the axial rotation vector $\boldsymbol{\omega}$,

$$\varepsilon = e + \omega = e - \boldsymbol{\omega} \times I, \tag{4.9}$$

$$\beta = -\operatorname{Rot} \varepsilon = -\operatorname{Rot} e + \frac{d\boldsymbol{\omega}}{d\mathbf{x}} - I \operatorname{div} \boldsymbol{\omega}, \tag{4.10}*$$

where I is the unit tensor. The diagonal terms of ϵ correspond to elastic elongation (compression), while the non-diagonal terms correspond to elastic shear, the first index corresponding to the plane of the shear and second to the direction of the shear.

It follows from (4.10) that the trace of β, corresponding to the total density of the screw dislocation, is determined by the divergence of the rotation vector, which in the presence of dislocations is no longer equal to zero:

$$\operatorname{Sp} \beta = -2 \operatorname{div} \boldsymbol{\omega}. \tag{4.11}$$

*Rot = curl.

The tensor $\kappa = d\omega/d\mathbf{x}$, which is the transpose of the tensor Grad ω describes the lattice curvature. If the lattice curvature and the microscopic elastic deformations of the crystal are determined by experiment (for example, from x-ray diffraction or optical measurements), relation (4.10) enables us to calculate the macroscopic density of the dislocations causing the given lattice distortion field.

If there are no macroscopic elastic strains (or stresses), then (4.10) and (4.11) lead to simple relations between the dislocation density and the lattice curvature·

$$\beta = \varkappa - I\,\mathrm{Sp}\,\varkappa; \quad \varkappa = \beta - \frac{1}{2} I\,\mathrm{Sp}\,\beta. \tag{4.12}$$

If the spherical components of the tensors β and κ vanish, the tensors themselves coincide. This consequence was used many times for an experimental check on the theory.

In ordinary elasticity theory we obtain from (4.10), in the absence of dislocations,

$$\frac{d\omega}{dx} = \mathrm{Rot}\, e \tag{4.13}$$

(div $\omega = 0$) or, in transposed form,

$$(\mathrm{Rot}\, e)^* = \mathrm{Grad}\, \omega. \tag{4.13'}$$

In order for the differential relation (4.13') to yield uniquely the rotation vector ω from the known deformations, the tensor (curl e)* must be potential. Putting

$$\mathrm{Rot}\,(\mathrm{Rot}\, e)^* = -\eta, \tag{4.14}$$

we obtain the Saint Venant compatibility conditions in the form $\eta = 0$, where η is the so-called strain incompatibility tensor.

In the presence of dislocations, Eqs. (4.10) and (4.14) lead to an expression for the strain incompatibility in terms of the macroscopic dislocation density [16]

$$\eta = \mathrm{Rot}\left(\beta^* - \frac{1}{2} I\,\mathrm{Sp}\,\beta\right) = \frac{1}{2}\left[\mathrm{Rot}\,\beta^* + (\mathrm{Rot}\,\beta^*)^*\right]. \tag{4.15}$$

Therefore the tensor β, like the incompatibility tensor, completely determines the internal stresses. We must, however, emphasize that it is wrong to attempt to determine the total dislocation density (4.7) and the plastic deformation from the tensor β.

To describe the motion of the dislocations, we need the third-rank tensor

$$N_{ijk} = \int (d\mathbf{b}) \int d\Omega\, v_i n_j b_k f_{\mathbf{b}}, \tag{4.16}$$

where $\mathbf{v} = \mathbf{v}(\mathbf{b}, \mathbf{n})$ is the velocity of dislocations having a direction $\mathbf{n}$ and a Burgers vector $\mathbf{b}$, with, of course, $\mathbf{v} \perp \mathbf{n}$.* In a simple cubic lattice, subject to the limitations indicated on p. 281, $k = i \neq j$ corresponds to gliding edge dislocations, $i \neq j = k$ corresponds to gliding screw dislocations, and $i \neq j \neq k \neq i$ corresponds to climb of edge dislocations.

The gliding of the dislocations produces plastic shear parallel to the glide plane and to the direction of the Burgers vector. Climb of the edge dislocations involves plastic contraction (or dilatation) of the crystal in the Burgers vector direction. In general the macroscopic plastic distortion ϵ^P is connected with the tensor of dislocation motion in the following fashion (see [32]):

$$\dot{\varepsilon}^P_{ij} = e_{mni} N_{mnj}, \tag{4.17}$$

hence

$$e_{ijl}\varepsilon^P_{lk} = (N_{ijk} - N_{jik}). \tag{4.17'}$$

Plastic distortion can be broken up into a symmetrical part, the tensor plastic deformations e^P, and an antisymmetrical part, which is the tensor of plastic rotations ω^P, equivalent to the rotation vector ω^P

$$\dot{\omega}^P_i = \frac{1}{2}(N_{jij} - N_{ijj}). \tag{4.18}$$

If the displacement of the dislocations is not uniform, dislocations accumulate within the crystal at a rate

$$\dot{\beta}_{jk} = -\frac{\partial}{\partial x_i}(N_{ijk} - N_{jik}). \tag{4.19}$$

The corresponding conservation equation for the distribution function has the form

$$\int (d\mathbf{b}) \int d\Omega\, b_k \left[\eta_j \left(\frac{\partial}{\partial t} + \frac{\partial}{\partial x_i} v_i\right) - n_i \frac{\partial}{\partial x_i} v_j\right] f_{\mathbf{b}} = 0. \tag{4.20}$$

Differentiating (4.17') with respect to the coordinate j, we obtain

$$\dot{\beta} = \mathrm{Rot}\, \dot{\varepsilon}^P. \tag{4.21}$$

If there are no dislocations in the initial state ($\epsilon^P = 0$), integration of (4.21) yields

$$\beta = \mathrm{Rot}\, \varepsilon^P. \tag{4.21'}$$

From a comparison of (4.10) and (4.21') it follows that the overall distortion is potential

$$\mathrm{Rot}\,(\varepsilon + \varepsilon^P) = 0. \tag{4.22}$$

Consequently, the summary distortion can be represented in the form of a gradient of a certain vector $\mathbf{u}$ (total displacement vector)

$$\varepsilon + \varepsilon^P = \mathrm{Grad}\, \mathbf{u}. \tag{4.23}$$

This is precisely the vector $\mathbf{u}$ involved in the equations of the dynamic theory of elasticity, which conserves its usual form

$$\rho \ddot{\mathbf{u}} = \mathrm{Div}\, \sigma \tag{4.24}$$

(ρ is the density of the material) even in the presence of moving dislocations.

*In the case of gliding dislocations, v is parallel to the edge component of the Burgers vector $\mathbf{n} \times \mathbf{b} \times \mathbf{n}$ and depends on the force acting on the glide plane in the b direction (i.e., on the tangential stress τ, acting on the glide plane in the glide direction). In the climb of dislocations, v is perpendicular to the glide plane and depends on the force acting in the b direction on the plane perpendicular to the edge component of the Burgers vector. In the case of quasi-viscous glide of the dislocations, when $\mathbf{v} = \mu\tau$, the dislocation motion tensor has the form

$$N_{ijk} = \int (d\mathbf{b}) \int d\Omega\, \frac{\mathbf{b}\sigma(\mathbf{b}\times\mathbf{n})}{(\mathbf{b}\times\mathbf{n})^2} \{b_i - n_i(\mathbf{bn})\} n_j b_k f_{\mathbf{b}}.$$

If there are no dislocations, we can find in accordance with (4.10) and (4.21′) the elastic displacement vector (as is usually done in elasticity theory) and the plastic displacement vector, respectively. In the general case these vectors do not exist, and only the total displacement vector can be determined.

With N_{ijk} specified, Eqs. (4.17), (4.19), (4.23), (4.24), and Hooke's law form the complete system of equations of the dynamic theory of elasticity for bodies with dislocations. If ϵ^P (or $\dot{\epsilon}^P$) is specified, Eqs. (4.17) and (4.19) in this system are replaced by (4.21′) or (4.21), respectively.

Hollander recently proposed a four-dimensional notation for bodies with moving dislocations.[33]

Nonlinear theory. When the crystallographic planes have appreciable curvature, it is necessary to take into account the distortion of the lattice metric. The corresponding nonlinear generalizations of dislocation theory were indicated by several authors (see the reviews in [19]). These employ the formalism of non-Riemannian geometry, with the tensor of local macroscopic dislocation density corresponds to a Cartan twisting of space

$$\beta^{ij} = e^{ikl}\Gamma^j_{kl}, \qquad (4.22')$$

where Γ^j_{kl} are the affine-connectivity coefficients.

Nonlinear effects of a different type should be taken into consideration when examining the stresses and strains near a dislocation nucleus,[34] where the elastic distortions are so great that they cannot be described by linear theory. An account of higher-order constants makes it possible to estimate correctly the decrease in crystal density due to the dislocations as well as other effects. The distortions in the nucleus of dislocation have an inelastic character and can be regarded only by using atomistic notions.

5. ATOMIC STRUCTURE OF DISLOCATIONS

In 1938 Frenkel and Kontorova first proposed an atomic dislocation model.[35] They considered the motion of chains of atoms, bound by quasi-elastic forces, on a rigid backing made up of similar chains, forming a periodic force field (Fig. 10). The equation of motion for the k-th atom has the form

$$m\ddot{\xi}_k = -\frac{\partial U}{\partial \xi_k} + \alpha(\xi_{k-1} + \xi_{k+1} - 2\xi_k), \qquad (5.1)$$

where ξ_k —displacement of the k-th atom from the equilibrium position, m —mass of the atom, α —coefficient of quasi-elastic coupling, $U = \sum_k \left(1 - \cos\frac{2\pi\xi_k}{b}\right)$ —force field. The displacement ξ is then regarded as a continuous function of k and a transition is made from the system (5.1) to the differential equation

$$m\ddot{\xi} = -\frac{\partial U}{\partial \xi} + \alpha\frac{\partial^2\xi}{\partial k^2}, \qquad (5.1')$$

which is solved under the assumption that the shear

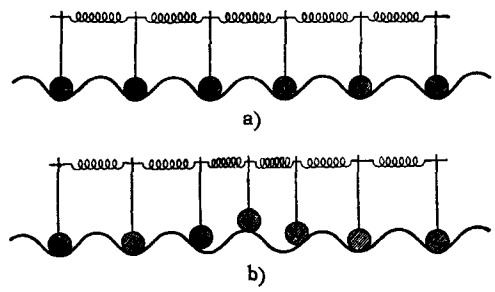

FIG. 10. The Frenkel-Kontorova model. a) Unperturbed state; b) edge dislocation (positive).

propagates gradually along the chain with constant velocity v, (i.e., uniform dislocation motion). In this case

$$\xi(k) = \frac{2b}{\pi}\operatorname{arctg}\exp\left[-\frac{\pi}{\lambda}(kb - vt)\right], \qquad (5.2)^*$$

where

$$\lambda = \frac{b^2}{2}\sqrt{\frac{\alpha}{A}}\sqrt{1-\frac{v^2}{c^2}} \qquad (5.3)$$

is the width of the dislocation, which experiences relativistic contraction as v approaches the velocity of sound $c = b\sqrt{\alpha/m}$. The dislocation energy is

$$\mathcal{E} = \frac{\mathcal{E}_0}{\sqrt{1-\frac{v^2}{c^2}}}, \qquad (5.4)$$

where

$$\mathcal{E}_0 = \frac{4b}{\pi}\sqrt{\alpha A}. \qquad (5.5)$$

Going over to macroscopic constants, the energy of the stationary dislocation per unit length amounts to about $0.3\,Gb^3$. The lowest energy is possessed by dislocations corresponding to slip in the closest packing directions. Estimating $\mathcal{E}_0$ from (5.5) for different slip directions in several metals, Frenkel and Kontorova observed a correlation between $\mathcal{E}_0$ and the experimental data on the plastic properties of these metals. Similar attempts to determine the directions of easy slip from the energy of the corresponding dislocations were made subsequently by many workers (see, for example,[36,37]). According to (5.4), the dislocation energy does not depend on the position of the center of the dislocation relative to the atoms of the backing, so that uniform motion of the dislocation does not necessitate the application of the external forces. Frenkel and Kontorova assumed that this conclusion that the slip of the chain is unhindered is connected with neglect of the displacement of the atoms in the backing. However, if the discrete nature of the chain is taken into account in calculating the dislocation energy, then the Frenkel–Kontorova model gives a finite resistance to slip even for an absolutely rigid backing, and this can be interpreted as the critical cleavage stress τ_k

*arctg = $\tan^{-1}$.

necessary for displacement of the dislocation.[38] When $v \ll c$, calculation yields an exponential dependence of τ_k on the width of the dislocation λ,

$$\frac{\tau_k}{G} = \frac{\pi\lambda}{3ab} \exp\left(-\frac{\pi\lambda}{b}\right), \tag{5.6}$$

where λ is proportional to a/b, where a is the interplanar distance. Consequently, the more tightly the atoms are located in the slip direction and the farther the slip plane is away from the neighboring planes, the greater the mobility of the dislocations. The well-known empirical rule for selecting the possible slip elements using the reticular density of the planes and directions, agrees precisely with this result. An estimate based on (5.6) shows that when $a = 2b$ the critical cleavage stress is vanishingly small, when $a = 0.5b$ it already reaches a very large value ($\tau_k \sim 0.004\,G$), and when $a \sim b$ it amounts to 10^{-5}—$10^{-4}\,G$, which is customarily observed in experiment.

Recently Kontorova generalized Eq. (5.1) by including the terms that are anharmonic in the interaction of the chain atoms, and traced the correlation between the plasticity and heat conduction.[39] In many investigations (see the reviews [15,17]) higher harmonics of the potential of the backing were taken into account, and, in particular, the conditions under which the dislocations dissociate were investigated. Indenbom and Kratokhvil used a potential U made up of parabolic and straight-line sections. In this case the system of difference equations (5.1) can be solved rigorously, and the resistance of the lattice to the motion of the dislocations is higher than would follow from (5.6), with τ_k reaching $6 \times 10^{-3}\,G$ for $\tau_0/G = 1/10$ and $6 \times 10^{-4}\,G$ for $\tau_0/G = 1/30$. The model of Eq. (5.1) was also extended to the two-dimensional case in [17].

The Frenkel–Kontorova model was applied also to other physical problems (epitaxy,[40] domain boundaries in ferromagnets,[41] interphase boundaries,[42] and inflexions on dislocations[43]).

A shortcoming of the Frenkel dislocation model is that only the short-range interactions in the atomic chain are taken into account. In fact, because of interaction with neighboring chains, long-range forces appear inside each chain, and a limiting transition to the theory of elasticity is impossible without an account of these forces. This shortcoming is eliminated in the Peierls–Nabarro model (see the review [15]), comprising two elastic half-spaces separated by a glide plane XY, in which the tangential stress τ is nonlinearly dependent on the difference between the tangential displacement u on both sides of the plane of separation

$$\tau = \frac{bG}{2\pi a} \sin\frac{2\pi u(x)}{b}. \tag{5.7}$$

The equation for elastic equilibrium of the half space, subject to boundary conditions (5.7), is

$$\frac{b(1-\nu)}{a} \sin\frac{2\pi u(x)}{b} = \int_{-\infty}^{\infty} \frac{du}{dx'} \frac{dx'}{x-x'}. \tag{5.8}$$

The dislocation is described by the solution

$$u(x) = \frac{b}{\pi} \operatorname{arctg}\frac{2(1-\nu)x}{a}, \tag{5.9}$$

which at large distances from the center of dislocation goes over into the solution of the theory of elasticity. The dislocation energy has a periodic dependence on the position of its center, and the resistance of the lattice to the motion of the dislocation corresponds to the critical cleavage stress

$$\tau_h = G \exp\left[-\frac{a}{2\pi(1-\nu)b}\right] \tag{5.10}$$

("Peierls force"). As in the Frenkel–Kontorova model, the dislocation energy is of the order of Gb^2, the mobility of the dislocation depends exponentially on its width, and the width is proportional to the ratio a/b. Different generalizations of the Peierls–Nabarro model (for screw dislocations, for anisotropic bodies, for specific crystal structures, etc) are given in the reviews [15,17].

In many works, the atomic structure of the dislocation was calculated by lattice-theory methods under different assumptions concerning the form of the potential of the interatomic interaction.[37,44] As a rule, the width of the dislocation is found to be very small, and the lattice resistance to the motion of the dislocation much higher than in the Frenkel-Kontorova and Peierls–Nabarro models. This discrepancy in the results is due not only to the crude models, but also to the substitution of differential equations for the difference equations under conditions when this procedure is not valid.*

6. MOBILITY OF DISLOCATIONS

The estimates given above for the static resistance of the lattice to the motion of dislocations are known to be too high, since they have been actually obtained under the assumption that the dislocation is directed exactly along the close-packing direction. Actually the dislocation may consist of segments located along the close-packing direction and joined by kinks (Fig. 11). In this case it is possible to overcome the potential barrier separating the neighboring troughs of the potential relief by moving of the kinks along the dislocation line. In the case of a sinusoidal potential relief

$$U = \frac{b^2\tau_k}{2\pi}\left(1 - \cos\frac{2\pi}{b}x\right), \tag{6.1}$$

where τ_k is the lattice resistance to the motion of dislocations without kinks (see Sec. 5), the form of the kink is described by the Frenkel–Kontorova equation

*According to[38], τ_k is determined by the Fourier spectrum $U[\xi(k)]$, and a sinusoidal relief $U(\xi)$ corresponds to the special case of an exponentially terminated spectrum. Recently I.M. Lifshitz investigated the solution of the system of difference equations (5.1) for an arbitrary smooth function $U(\xi)$ and established that τ_k falls off with increasing dislocation width λ not exponentially, but as λ^{-5}.

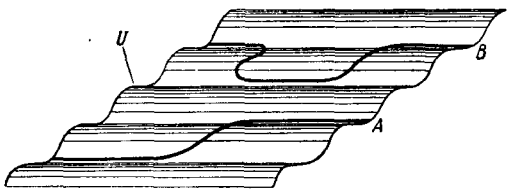

FIG. 11. Kinks on dislocations. A – Single kink; B – double kink; U – lattice potential field relief.

$$\mathscr{E}_0 x'' = b\tau_k \sin\frac{2\pi}{b}x - b\tau. \qquad (6.1')$$

Here $\mathscr{E}_0$ –linear dislocation energy, τ –external shear stress acting on the glide plane in the glide direction. According to Seeger et al [43] the width of a single kink is $\Lambda_0 = \sqrt{\pi\mathscr{E}_0/2\tau_k}$, the energy of a single kink is $W_0 = 4\Lambda_0 b^2\tau_k/\pi^2$, the length of a double kink is $\Lambda \approx (\Lambda_0/\pi) \times \ln(16\tau_k/\pi\tau)$, etc.

Thermal fluctuations give rise to double kinks, some of which are immediately annihilated, but some survive and migrate along the dislocation with speed $v_0 \approx c\tau b^3/kT$ (Lothe et al [43]), until they are annihilated by kinks coming from the opposite direction. The speed of the dislocation is

$$v = 2nbv_0, \qquad (6.2)$$

where n is the running density of the kinks surviving at a given level of stresses.

Lothe and Hirth [43] considered such cases of internal friction and creep, in which n was limited by the annihilation by opposing kinks. Calculation of the partition function yielded the estimate

$$n \approx \frac{1}{b}\left(\frac{b^3\tau_k}{kT}\right)^{1/2}\left(\frac{2\pi b^2\tau_k}{\mathscr{E}_0}\right)^{1/4}\exp\left(-\frac{W_0}{kT}\right). \qquad (6.3)$$

It follows from the condition (6.2) that in this case the speed of the dislocations is proportional to τ, and the activation energy of the process is independent of the stress.

As τ increases, the stress dependence of the probability of creation of stable kinks manifests itself more and more strongly, and the function $v = v(\tau)$ becomes nonlinear. As τ approaches τ_k, the number of stable kinks should increase rapidly, while the speed of the dislocations approaches the speed of the kinks.

At large dislocation speeds, the resistance of the lattice is determined not so much by the potential relief as by the different dynamic effects. Even Frenkel and Kontorova [35] pointed out the important role of momentum transfer from the dislocation to the surrounding lattice. In their model this corresponded to an account of the mobility of the backing atoms. It was assumed that the atoms of the backing are capable of fluctuating about their equilibrium positions independently of each other, with frequency ω, and are excited by the passing dislocation. The energy lost by the dislocation is equivalent to a resistance

$$\tau_F = \frac{ma}{2b^*}\left(\frac{c^2}{v^2}-1\right)^2\frac{\omega^2}{\mathrm{ch}^2\frac{\pi\omega\lambda}{2v}}, \qquad (6.4)^*$$

where b* is the lattice parameter along the dislocation; for the other symbols see Sec. 5. The resistance to the motion of the dislocation tends to zero for both slow and very fast dislocations.

Leibfried and Nabarro considered the dislocation-to-lattice momentum transfer due to scattering of phonons. [45] In this case the principal role is played by the nucleus of the dislocation; where the superposition of the elastic waves and the field of dislocation is disturbed. The effective resistance of the lattice is proportional to the speed of the dislocation. A simplified estimate (without account of the reduction in the cross section during the scattering of long-wave phonons) yields

$$\tau_s \approx \frac{1}{10}\frac{v}{c}\bar{\varepsilon}, \qquad (6.5)$$

where $\bar{\epsilon}$ is the density of the thermal-oscillation energy.

When the speed or form of the moving dislocation changes, its elastic field is also changed and elastic waves are radiated as a result. The corresponding radiation friction τ_R is completely analogous to radiation friction in electrodynamics. In particular, the problem of radiation of elastic waves by a screw dislocation is equivalent to the problem of radiation of electromagnetic waves by a charged filament. [27] Radiation friction in the motion of the dislocation in a periodic lattice field was investigated by Seeger and Burchhardt ([17], p. 623). An estimate of the amplitudes of the oscillations in the speed of dislocation, made for the Frenkel–Kontorova and Peierls–Nabarro models, has shown that τ_R reaches an appreciable value (on the order of 10^{-4} G) only when $v/c \sim 0.2$–0.4. Radiation friction connected with the forced oscillations of the dislocation under the influence of phonons (thermal fluctuations) turns out to be even smaller. This effect, unlike slowing down due to phonon scattering, is proportional to v^2/c^2. [45]

For rapidly moving dislocations we can also expect emission of elastic waves by the Vavilov–Cerenkov mechanism. An edge dislocation should obviously radiate transverse waves over the entire spectrum if its velocity is intermediate between the velocities of the transverse and longitudinal waves. Eshelby has noted [46] that since the velocity of the short-wave lattice oscillations can be half as large as that of the long-wave oscillations (the velocity of sound), a screw dislocation moving with a velocity $v > c/2$ is "supersonic" for part of the oscillation spectrum. One can assume that this mechanism determines the maximum attainable speed of the dislocation.

Many slowing-down mechanisms are connected

*ch = cosh.

with relaxation phenomena in the field of the moving dislocation. The motion of the dislocation is accompanied by a local increase in the temperature in the compression regions of the crystal and a decrease in temperature in the dilatation regions. The transfer of heat from the compressed to the dilated regions leads to dissipation of energy (thermoelastic friction). According to Eshelby[47] the thermoelastic effect corresponds to a very small lattice resistance

$$\tau_T \cong 10^{-5} G \frac{v}{c}. \qquad (6.6)$$

More appreciable relaxation losses are connected with the motion (displacement, reorientation, etc) of point defects. In particular, in solid solutions a local change in the order takes place in the vicinity of the dislocations.[48] The corresponding lattice resistance is small for slow dislocations (the region of local ordering does not lag the dislocation) and very fast dislocations (there is not time at all for the ordering to take place).

A local change in the concentration of the impurity atoms near the dislocation can lead to enforcement of the remaining dislocations.[49] To tear away a dislocation from a cloud of impurity atoms (Cottrell cloud) it is necessary to overcome the forces of interaction between the atoms and the dislocation, which can be of different nature. The rupture stress is

$$\tau \approx \frac{V}{b^3}, \qquad (6.7)$$

where V —energy of the bond between the impurity atom and the dislocation. At lower stresses the dislocation is forced to migrate together with the Cottrell cloud. A rough estimate[49] yields for the lattice resistance in this case

$$\tau \approx \frac{10 c_0 V^2}{kTDb^2} v, \qquad (6.8)$$

where c_0 —atomic concentration and D —coefficient of impurity atom diffusion.

The relaxation motion of other dislocations in the field of the moving dislocation gives an energy dissipation equivalent to the effective increase in the path covered by the moving dislocation. The slowing down of the dislocation by the relaxation motion of surface defects that do not reduce to dislocation networks (grain boundaries, ferromagnetic and ferroelectric domains, ordering regions, etc) can also be estimated if the relaxation mechanism is known.

Finally, the relaxation slowing down can also be connected with the motion of atoms in the dislocation core. The resistance to the motion is given by the Einstein formula

$$\tau_D = \frac{kT}{b^2 D^*} v, \qquad (6.9)$$

where D* is the effective coefficient of diffusion of the atoms in the nucleus.[50]

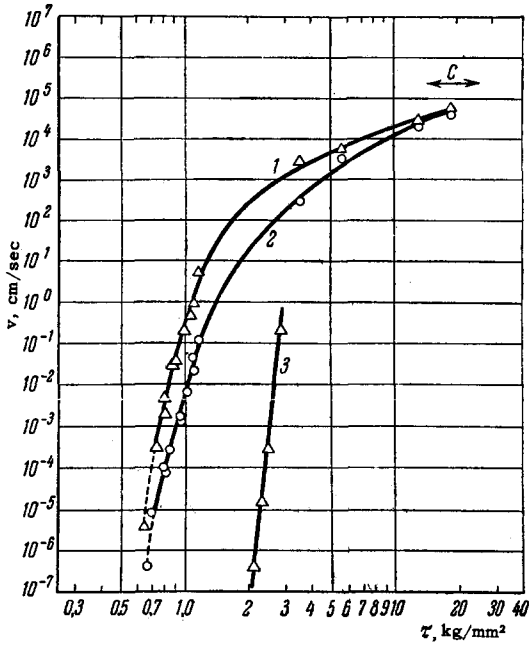

FIG. 12. Mobility of dislocations in crystals. 1 – Edge dislocations at 300°K; 2 – screw dislocations at 300°K; 3 – screw dislocations at 77°K.

Experimental data on the mobility of dislocations were obtained only recently. The most interesting are the results of Gilman and Johnston,[51,52] who investigated by selective etching the speed of dislocations in LiF crystals as a function of the stress. Figure 12 shows the $v(\tau)$ curves for 77 and 300°K. Motion of dislocations with noticeable velocity begins at stresses on the order of the macroscopic yield point. Increasing the stress by less than two orders of magnitude causes the speed to increase by 11 orders and to reach approximately 0.1 c.

So weak a dependence of τ on v is apparently evidence that the resistance to the motion of dislocations is determined in this case not by dynamic but by static effects (overcoming certain potential barriers). As can be seen from Fig. 12, a change in temperature brings about a parallel shift of the curve along the "log v" axis, so that we can estimate the activation energy W, which amounts to about 0.7 eV at $\tau = 1$ kg/mm². For a screw dislocation, the $v(\tau)$ curve can be well approximated by the formula*

$$v = 10^5 \cdot \exp\left(-\frac{16.8 \cdot 10^8}{\tau}\right) \qquad (6.10)$$

(τ and v are in cgs units). We note that a $W \sim \tau^{-1}$ relation is characteristic of processes connected with nucleation (for example, the speed of domain boundaries in ferroelectrics as a function of the electric field intensity). Bombardment of crystals by neutrons, and

*However, Eq. (6.10) leads to W = 0.4 eV in place of W = 0.7 eV at $\tau = 1$ kg/mm². This contradiction is apparently eliminated if the experimental data are reduced by formulas similar to (6.2).

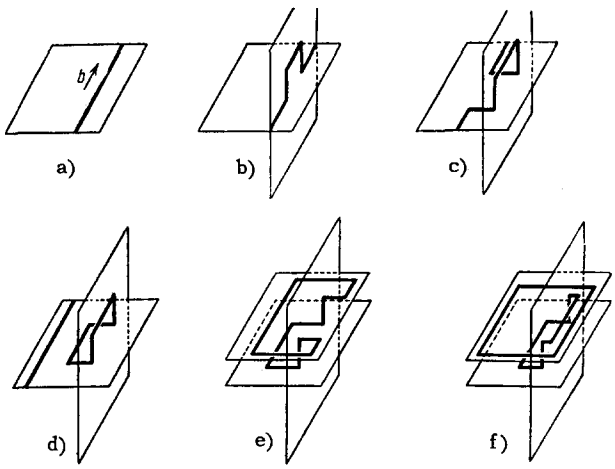

FIG. 13. Multiplication of dislocations by double cross slip. a) Screw dislocation in initial glide plane; b) portion of dislocation shifted along the cross-slip plane; c) dislocation continues to move forward, vertical segments remain in place; d) dislocation broke away and left behind it a loop lying in two intersecting planes; e–f) one of the horizontal portions of this loop detaches new loops, as in a Frank-Read source.

also prior plastic deformation, shift the $v(\tau)$ curve in the same direction as a decrease in the temperature. In the latter case the shift of the curve along the τ axis agrees satisfactorily with the theoretical estimate of the amplitude of the field of internal stresses produced by the dislocations formed during the plastic deformation.

7. PLASTIC DEFORMATION AND HARDENING

During the course of plastic deformation, appreciable changes, due to the interaction of the dislocations among themselves and with other lattice defects, take place in the dislocation structure of the crystal. Theory predicts a large number of possible mechanisms for such interactions. Many have already been experimentally confirmed. But theory cannot point out with certainty the precise mechanism that governs the plastic deformation process in each specific case. Consequently further progress in the physical theory of plasticity is dependent on the results of direct experimental research on the mechanism of plastic deformation in different materials and under different conditions.

We discuss below only the main aspects of dislocation theory of plasticity.

Dislocation sources. To produce in the crystal enough dislocations for plastic deformation and to compensate the loss of dislocations by emergence to the surface (and by annihilation inside the crystal), dislocation sources must be present. Until recently it was assumed that the main sources of dislocations were segments of the dislocation network that sag gradually under the action of the stresses, until they lose mechanical stability and a new dislocation loop

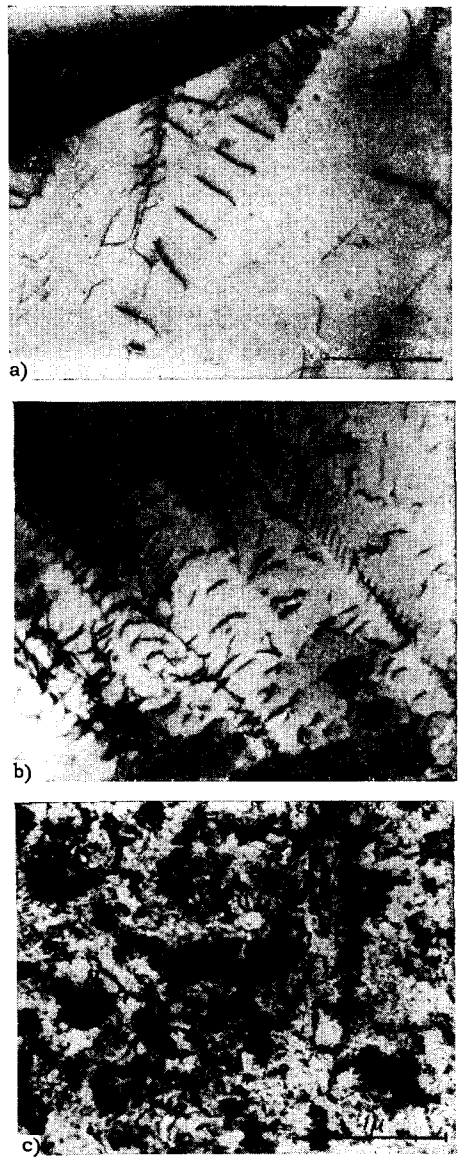

FIG. 14. Dislocation structure of stainless steel after deformation by 1% (a), 8% (b) and 96% (c). a) Flat accumulation of dislocations appeared at the grain boundary; b) these accumulations crossed dislocations of other slip systems and hexagonal configurations were formed in many places; c) dense accumulations of intertwining dislocations.

is detached (Frank–Read source [53]). Such sources were indeed observed experimentally in silicon, potassium chloride, stainless steel, cadmium, and other metals. However, the mechanism wherein dislocations are multiplied with the aid of Frank–Read sources turned out to be not as universal as assumed. Johnston and Gilman [54] found that dislocations moving in LiF crystals create new loops directly via double cross-slip (Fig. 13), in accordance with a mechanism which was proposed earlier by Orowan. [55] Multiplication of dislocations by this mechanism, and also the detachment of loops from large jogs on moving dislocations, was observed in different metals in a transmis-

sion electron microscope. Etching, decoration, and direct electron-microscopic observation have disclosed in various materials the creation of dislocations on inclusions, precipitates, and other stress concentrators. The occurrence of dislocation loops by collapse of flat accumulations of point defects, produced during the quenching of metals, was investigated in detail. The mechanism whereby dislocations are produced by grain boundaries, with emergence of half-loops to one side of the boundary, frequently observed in the electron microscope, has been neither predicted nor so far explained. This case should be accompanied by changes in the dislocation density in the boundary.

Hardening. The density of dislocations and point defects increases in the course of the plastic deformation. Figure 14 shows by way of an example the dislocation structure of stainless steel at different stages of plastic deformation.[56]

If Q sources per unit volume each emit n loops of radius R, the attained plastic deformation is

$$e = \pi R^2 Q n b, \tag{7.1}$$

and the dislocation density increases by

$$N = 2\pi R Q n. \tag{7.2}$$

If the radius of loop divergence is constant, the relation between e and N is linear:

$$N = \frac{2}{bR} e. \tag{7.3}$$

The proportionality of N and e was observed experimentally in single crystals of LiF,[51] where N $= 10^9$ e, in polycrystalline silver[57] ($N = 2 \times 10^{11}$ e), and in other materials. According to (7.3), the divergence radius is 7×10^{-2} cm in LiF and 7×10^{-4} cm in silver. In LiF, the divergence radius is equal to the dimension of the experimentally observed large loops, while in silver it exceeds by several times the diameter of the substructure cells, which were separated by dense networks of dislocations.

If the loops are emitted by sources with constant frequency ν and diverge with constant radial velocity v, the plastic deformation increases in accordance with (7.1) as the cube of the time

$$e(t) = \pi v^2 Q \nu b t^3. \tag{7.4}$$

Such a dependence was observed at the initial stage of plastic deformation of single crystals of germanium, and was maintained until the frontal dislocations reached the free surface of the crystal, after which N stopped growing and the deformation increased linearly with t.[58]

Plastic deformation leads not only to an increase in the total dislocation density, but also to an increase in the number of jogs on the dislocations, owing to the mutual crossing of the dislocations.

The range of the dislocation loops is determined by the obstacles of various types, most frequently grain boundaries and sitting dislocations, arising as a result

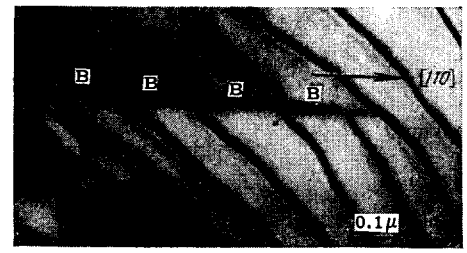

FIG. 15. Series of Lomer-Cottrell barriers (B) occuring along the line where a flat accumulation of dislocations crosses dislocations from another slip system; alloy Ni + 4% Al.[59]

of the dislocation reactions. The reactions that lead to the formation of barriers were analyzed in detail for the fcc lattice,[59] in which the splitting of the dislocations in the intersecting slip planes can merge into sitting dislocations of complicated structure, which block both slip planes simultaneously. The best known obstacles of this type are the Lomer–Cottrell dislocations[49] occurring in the reaction $\frac{1}{2}[110] + \frac{1}{2}[0\bar{1}1] = \frac{1}{2}[101]$ with unification of only the frontal partial dislocations, in accordance with the reaction $\frac{1}{6}[21\bar{1}] + \frac{1}{6}[\bar{1}\bar{1}2] = \frac{1}{6}[101]$, and formation of a V-shaped stacking fault along the edge $[10\bar{1}]$ (Fig. 15). Other similar reactions can produce, in accordance with [59], stronger barriers.

If the dislocations produced in the course of plastic deformation are distributed at random, the amplitude of the internal-stress field produced by them is approximately equal to $(1/2\pi)\,Gb\sqrt{N}$. For the plastic flow to continue it is thus necessary to increase continuously the applied stress σ in accord with the increase N. In the case of condition (7.3) we have for $\tau \simeq \sigma/2$

$$d\sigma = \frac{1}{2\pi} Gb\, d\sqrt{N} = \frac{G}{\pi}\sqrt{\frac{2b}{R}}\, d\sqrt{e}, \tag{7.5}$$

from which we obtain the usual quadratic hardening law for polycrystals

$$\sigma = \sigma_0 + AG\sqrt{e}, \tag{7.6}$$

where $A \sim \sqrt{b/R}$.

If the dislocations emitted by different sources are not distributed at random but form accumulations of n dislocations of the same sign, then the structure of the internal-stress field will be different. Each dislocation of the accumulation will counteract the work of the source with a stress on the order of Gb/R, so that $d\sigma \simeq (Gb/R)\,dn$. Taking (7.1) into consideration, we obtain

$$d\sigma = \frac{Gb}{R}\frac{de}{\pi R^2 Q b}. \tag{7.7}$$

When the number of sources M inside a sphere of radius R is constant, (7.7) yields a linear law of hardening with a hardening coefficient $\sim G/M$. In fcc metals, for example, linear hardening is observed in the first two stages of plastic deformation,* and in the

*Three main stages are distinguished on the strain curves of fcc metals: easy slip (I), fast hardening (II), and dynamic recovery (III).

second stage $M \approx 300$ for all metals and depends very little on the orientation of the crystal and on the temperature.[60] Usually the hardening in the second stage is attributed to accumulations of dislocations near the Lomer–Cottrell barriers.[60] However, the experimental data can also be explained by the slowing down of the dislocations by the jogs. If m is the linear concentration of the jogs on the dislocation, and $U = \alpha Gb^3$ is the energy needed to produce a point defect, then the stress required to move the dislocations without thermal activation is

$$\tau = \frac{mU}{b^2} = \alpha m G b. \tag{7.8}$$

The number of intersections generating the jogs is proportional to the deformation. Therefore, so long as the jogs are not annihilated, $m \sim e$ and (7.8) gives linear hardening. Under certain assumptions it becomes possible to explain the observed value of the hardening coefficient.[61]

Recovery. Simultaneously with the strain hardening, thermally activated recovery processes develop during the course of plastic flow: the dislocation accumulations diffuse, dislocations of opposite signs annihilate each other, and unlike jogs on the dislocations annihilate each other. As the stress increases, the activation energy $W(\sigma)$ of these processes decreases. When the rate of recovery increases rapidly, a sharp decrease takes place in the rate of hardening and a changeover to the next stage of plastic deformation occurs. The temperature and velocity dependences of the critical stress σ_k corresponding to this transition are determined from a relation of the type

$$\dot{e} \sim \exp\left(-\frac{W(\sigma_k)}{kT}\right). \tag{7.9}$$

For example, in an fcc metal the transition to stage III of the deformation is connected apparently with the diffusion of the dislocation accumulations by cross-slip. The activation energy of the cross-slip of the split dislocations is determined by the energy of the stacking fault and depends logarithmically on the stress.[62] In crystals with a diamond lattice, the transition from stage II to stage III is explained by the emergence of the dislocations from the accumulation by climbing, which in this case is more probable than cross slip.[63]

Another example of recovery is the annihilation of jogs on the dislocation lines. This process can be described by means of a kinetic equation of the type

$$\dot{m} = N_0 v - v_c m^2, \tag{7.10}$$

where N_0 is the density of the dislocation "forest," crossed by the moving dislocation, v_c —speed of migration of the jogs along the dislocation. From (7.10) we get $m = m_\infty \tan^{-1}\sqrt{Nvv_c}\, t$, where $m_\infty = \sqrt{Nv_c/v}$ is the limiting jog density. The corresponding plastic-flow stress can be estimated from (7.8). An analysis of the complete picture of hardening and recovery of specific crystals is beyond the scope of the present review. The main theoretical and experimental data on the mechanism of plastic deformation of the most thoroughly studied crystals can be found in the original papers and reviews, which cover fcc metals,[60,61,57] hexagonal metals,[64] germanium,[63,58] ionic crystals,[52] and the simple cubic lattice (theoretical model).[31] Abundant material on metals, ionic crystals, and crystals with diamond lattice is contained in a recently published book[65] which, like the book[49], contains also fundamental information on the mechanism of plastic deformation of heterogeneous crystals, which are of great practical interest. The laws of plastic flow of polycrystals (if slip along the grain boundaries does not play an appreciable role) reduce to the corresponding laws for single crystals.[66] Experimentally one usually obtains the following dependence of the plastic-flow stress σ on the grain diameter d:

$$\sigma = \sigma^* + kd^{-1/2}. \tag{7.11}$$

The quantity σ^* characterizes the resistance of the crystal to the motion of the dislocations. The difference $\sigma - \sigma^*$ determines the effect of stresses that press the dislocations against the grain boundary. In order for the theoretical strength $(G/2\pi)$ to be attained as a result of the concentration of stresses on the end of the slip line (concentration coefficient $\sqrt{d/b}$), the condition (7.11) with $k \sim G\sqrt{b}/2\pi$ must be satisfied. This estimate of k gives satisfactory agreement with experiment.

8. FAILURE

In discussing the low strength of ordinary materials, J. I. Frenkel believed that the experimental value of "rupture stresses" corresponds to the development of already existing cracks. According to Griffith, the dimension l^* of these cracks can be estimated from energy considerations. For example, a through crack of length l in a plate of thickness h has a surface energy $2h\gamma l$ (γ —surface energy) and reduces the elastic energy of the body in a field of stresses σ by an amount $\sigma^2 h l^2/2E$. The additional energy connected with the presence of the crack has a maximum when $l = l^* = 2\gamma E/\sigma^2$. When the stress is larger than σ, a crack with dimension $l \geq l^*$ develops without obstacles, and this causes fracture of the body.

While accepting Griffith's treatment of the magnitude of the destructive stresses, Frenkel noted several shortcomings in the theory. When $l < l^*$ the crack should close up spontaneously. The irreversibility of the lengthening of the crack can be explained only by assuming in addition that after the crack opens up the surface energy γ is decreased by adsorption of surface-active substances (the Rebinder effect). Account must also be taken of the dependence of the surface energy on the width of the crack. This dependence

causes the width of the crack to drop gradually to zero on approaching the edge, i.e., the crack does not have an elliptical form, but ends in a sharp corner. Emphasizing, finally, that Griffith's theory does not even raise the question of the origin of the generating cracks, Frenkel pointed out in this connection the work of A. V. Stepanov, who stated that the generation of the cracks was not spontaneous, but resulted from the plastic deformation that preceded the brittle fracture and depended essentially on the anisotropy of the crystal.

At the present time, Frenkel's outline of a theory of failure has been realized to a considerable degree. For differently-shaped cracks developing in an arbitrary stress field, it was possible to calculate the configuration force F acting on the corner of the crack, and equal to the gain in elastic energy as the corner moves through a unit length.[67,68] Thus, in the planar case, for a crack located at the plane y = 0 between the lines $x = x_1$ and $x = x_2$, the force acting on the corner $x = x_1$ is

$$F = \frac{\pi (x_2 - x_1)}{4G} [\bar{\tau}_{yz}^2 + (1 - \nu)(\bar{\sigma}_{yy}^2 + \bar{\tau}_{xy}^2)], \ldots, \quad (8.1)$$

where the bar denotes the weighted mean stress acting prior to the opening of the crack on the segment (x_1, x_2)

$$\bar{\sigma}_{iy} = \frac{2}{\pi (x_2 - x_1)} \int_{x_1}^{x_2} \sigma_{iy}(x') \sqrt{\frac{x_2 - x'}{x' - x_1}}\, dx'.$$

Equating the configuration force to twice the surface tension we obtain the condition for equilibrium of the crack

$$F = 2\gamma, \quad (8.2)$$

where γ stands for the surface energy not at the corner, but in the central part of the crack. Therefore the dependence of γ on the width of the crack influences the energy only in the case of very narrow cracks. To the contrary, the shape of both narrow and broad cracks depends essentially on the law governing the decrease of γ with increasing width of the crack. This problem has been considered both within the framework of elasticity theory[69] and for the atomic model.[70]*

The mathematical apparatus of the theory of dislocations can be successfully used to describe cracks, with the discontinuities replaced by suitably placed dislocations.[68]

The experimental researches have shown that the development of a crack is accompanied as a rule by intense plastic deformation near the corner of the crack. This leads to an effective increase in the surface energy (sometimes by one order of magnitude and more) and to irreversibility of the spread of the crack. Much experimental and theoretical data has been accumulated on the effect of surface-active substances on failure (see the reviews [73]). It can be assumed that the observed decrease in the work of rupture, resulting from the addition of certain impurities, is connected not only with the reduction in the surface energy, but also with the easing of the plastic deformation that accompanies the development of the crack. A correlation was also noted between precipitation and the reduction in the strength due to addition of an impurity. A calculation of the kinetic energy connected with the opening of the crack enables us to explain the experimentally observed stress dependence of the speed of propagation of the crack.[74]

The most significant progress has been attained recently in the investigation of the problem of initiation of cracks. Dislocation theory considers several atomic mechanisms for the initiation of cracks, which are essentially realizations of Stepanov's idea[75] that failure is initiated in places where plastic deformation proceeds unevenly. Both geometric and force models were investigated. In the former case the continuity of the crystal is destroyed as a result of the unification of chains of vacancies, generated by jogs on the moving dislocations.[76] This results in an initiating crack with an obtuse corner (on an atomic scale) (Fig. 16a). In the second case, the cracks are formed in regions where there are large internal stresses due to the dislocations. The crack produced has a sharp corner (Fig. 16b). As can be seen from Fig. 16, geometrical cracks are more stable than force cracks. When the former cave in, additional work must be expended to form the dislocation loop (prismatic dislocation) along the contour of the crack.

The most important variants of formation of force cracks are illustrated in Fig. 17 a–f. The variant most frequently discussed in the literature is a) —uncompleted shear, i.e., the accumulation of dislocations in front of an obstacle.[77] The only possible sufficiently strong obstacles are, apparently, the grain boundaries, so that in single crystals the realization of such a scheme has little likelihood. Unfortunately, many authors use indiscriminately the scheme of Fig. 17a to "explain" the fracture of single crystals. In polycrystals, the scheme of Fig. 17a gives a dependence of the rupture stress on the grain diameter similar to (7.11), with $k \sim \sqrt{\gamma G}$, which is in good agreement with experiment (see the review [77]).

It was observed that in hexagonal polycrystalline metals, incompleted shear at grain boundaries causes failure not in accordance with scheme a), but on the accumulation plane (Fig. 17b).[78] Gilman attributes this type of failure to local lattice expansion resulting from nonlinear effects in the dislocation core (see Sec. 4). It is more probable that the failure is due in this case to shear along the bent glide planes (see Fig. 17c)[68] —a geometric glide nonlinearity in the curved lattice. The limiting case of the scheme of

*Frenkel attempted to determine the dependence of the surface energy on the thickness of the crack, but was unable to complete the work, having discovered a mistake in the calculations. Unfortunately, this mistake remained uncorrected in the posthumous edition of[71]; see also[72].

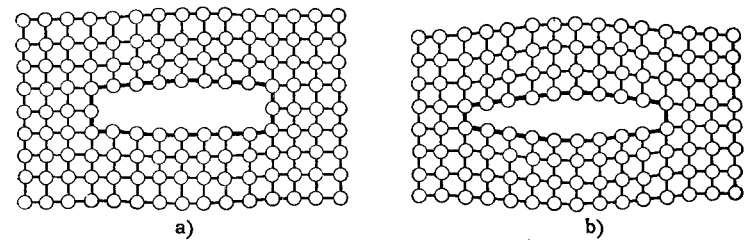

FIG. 16. Types of initiating cracks. a) 'Geometrical' crack; b) 'force' crack. After subtracting the elastic displacements, the thickness of crack (b) is equal to zero, while that of (a) differs from zero.

Fig. 17c is rupture of a block boundary (Fig. 17d) either as a result of crossing of the boundary by an active glide plane, or as a result of stoppage of part of the moving boundary, or finally, as a result of division of the boundary into parts as its orientation changes.[68,79] The configuration of Fig. 17d was observed experimentally in various crystals, in which the glide plane coincides with the cleavage plane (zinc, napthalene, and others). Accumulations of dislocations on the intersection of the glide planes can cause cracks in accordance with the scheme of Fig. 17e.[80] Cracks on the intersection between glide lines were observed frequently in crystals with MgO lattice, but the dislocation structure did not always correspond to the scheme of Fig. 17e. Failure in accordance with the scheme of Fig. 17f was recently observed in cadmium,[81] where the initiating crack occurred in a region where tensile stresses from two dislocation accumulations of opposite sign were superimposed. Judging from all data, the schemes of Fig. 17 do not cover all the possible dislocation mechanisms of generation of cracks. (See, for example, the ideas advanced by Oding[82] concerning the role of dislocations in the generation and development of cracks in metals.) One can expect that the most difficult cases of generation of cracks in crystals will be investigated in the near future both theoretically and experimentally.*

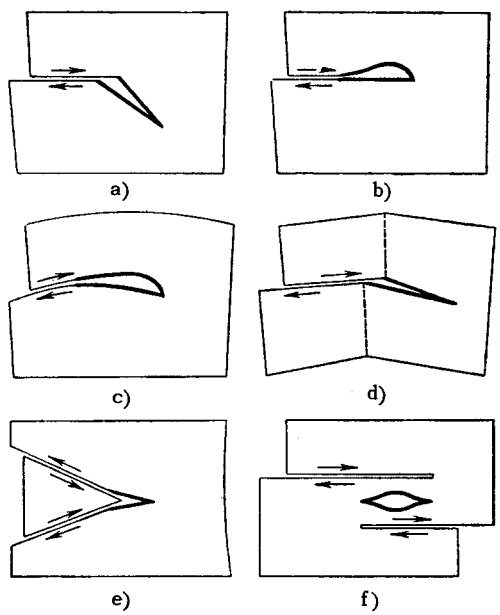

FIG. 17. Different variants of crack generation. a) Uncompleted shear after Zener-Mott; b) uncompleted shear after Rozhanskiĭ and Gilman (cleavage of accumulation of dislocations); c) crack in the glide plane as a result of shear in a curved lattice; d) rupture of vertical wall of dislocation; e) crossing of glide planes; f) crack between accumulations of dislocations of opposite sign.

The main problem in the theory of failure is now the atomic mechanism of propagation of cracks. According to Zhurkov and Sanfirova,[84] the endurance τ_σ (lifetime of the material under load) is inversely proportional to the steady-state creep rate and is well described by the formula

$$\tau_\sigma \sim \exp\left(\frac{U-\Omega\sigma}{kT}\right). \qquad (8.3)$$

It is still unclear whether the rate of failure is determined by the rate of creep or vice versa.[85] The authors of the survey hold opposite opinions on this subject (compare [85] with [68]).†

The development of the atomic mechanism of generation of propagation of cracks does not solve the problem of the statistical character of failure, to which J. I. Frenkel attached great significance.[86] The physical theory of failure should, of course, explain not only the average strength of a body with given structure, but also the strength distribution curve, the scale factor, and other regularities that necessitate a statistical approach to the account of the role of defects. A solution of this problem calls for a discovery of the physical meaning of the functions and the parameters that are involved in the statistical theory of strength. At the present time only the first steps have been made in this direction (see [87] and also the book [88]).

9. CONCLUSION

In 1950, J. I. Frenkel wrote (see [11], p. 364): "In spite of the prolonged study of mechanical prop-

*In polymers, the crack is frequently not merely a break in the continuity, but a cavity braced by chains of unbroken bonds. In the investigation of the strength of a body it is appropriate to use in this case the model of a single-dimensional atomic chain.[89]

†According to Zhurkov, the activation energy U greatly exceeds the activation energy of self diffusion U_D and is approximately equal to the evaporation energy U_0. However, one can just as well set the value of U in correspondence with the activation energy for the creation of interstitial atoms, which is close to U_0. In this case the rate of creep and of failure is limited by the creation of the interstitial atoms. The activation volume Ω can be set in correspondence with the quantity $b^2 l$, where l is of the order of the distance between dislocations (b/l is of the order of the angle of disorientation of the blocks).

erties of solids, particularly their plasticity, this question has to this very day not only failed to receive correct solution, but could not even be correctly formulated. It can be stated that the introduction of mobile dislocations and of a theory for their motion was a first step towards solving the problem of plastic deformation and hardness of crystals. At the present time, however, there is still very little done towards further development of the theory of plasticity and its specific applications to particular bodies."

During the last decade the dislocation hypothesis has found brilliant experimental confirmation, while dislocation theory has become an inseparable part of solid state theory. But while the principles of dislocation theory can be regarded as developed, the same cannot be said concerning the dislocation theory of plasticity and strength. The development of clear ideas concerning the atomic mechanism of plastic flow and failure still calls for extensive experimental and theoretical research.

Modern advances in experimental methods of the study of defects in crystals enable us to hope that a solution of this problem will not be long in coming.

[1] J. I. Frenkel, Z. Physik **37**, 572 (1926).

[2] Cited by Cottrell [49], p. 22.

[3] S. S. Brenner, Growth and Perfection of Crystals, Wiley, New York, 1958, p. 157.

[4] Nadgornyĭ, Osip'yan, Perkas, and Rozenberg, UFN **67**, 625 (1959), Soviet Phys. Uspekhi **2**, 282 (1959).

[5] J. I. Frenkel, Z. Physik **35**, 652 (1926); Kinetic Theory of Liquids, Dover, N. Y. 1954.

[6] Seeger, Schiller, and Kronmüller, Phil. Mag. **5**, 853 (1960).

[7] Gibson, Goland, Milgram, and Vineyard, Phys. Rev. **120**, 1229 (1960)

[8] E. W. Müller, Z. Physik **156**, 399 (1959).

[9] A. J. Forty, Direct Observation of Dislocations in Crystals (Russ. Transl.) Moscow, Metallurgizdat, 1956; Regel', Usovskaya, and Kolomiĭchuk, Kristallografiya **4**, 937 (1959), Soviet Phys. Crystallography **4**, 895 (1960). W. Dekeyser and S. Amelinckx, Solid State Phys. **8**, 325 (1959); A. R. Lang, J. Appl. Phys. **30**, 1748 (1959); P. B. Hirsch, Metallurg. Rev. **4**, 101 (1959); M. V. Klassen-Neklyudova and V. L. Indenbom, Editor's article in collection "Dislocation and Mechanical Properties of Crystals" Moscow, IL, 1960.

[10] A. N. Orlov and I. A. Shvarte, FMM (Physics of Metals and Metallography) **10**, 492 (1960).

[11] J. I. Frenkel, Introduction to the Theory of Metals, 3d. ed. Fizmatgiz, 1958.

[12] F. R. N. Nabarro, Conf. on Strength of Solids (Phys. Soc., London, 1948), p. 75; C. Herring, J. Appl. Phys. **21**, 437 (1950).

[13] V. M. Rozhanskiĭ and V. M. Stepanov, DAN SSSR **133**, 804 (1960), Soviet Phys.-Doklady, **5**, 831 (1961).

[14] Whelan, Hirsch, Horne, and Bollmann, Proc. Roy. Soc. **A240**, 524 (1957).

[15] F. R. N. Nabarro, Advances Phys. **1**, 269 (1952).

[16] E. Kröner, Kontinuumstheorie der Versetzungen und Eigenspannungen, Springer, Berlin, 1958.

[17] A. Seeger, Handb. Phys. **7**(1), 383 (1955).

[18] J. D. Eshelby, Solid State Phys. **3**, 79 (1956); R. de Wit, Solid State Phys. **10**, 249 (1960).

[19] E. Kröner and A. Seeger, Arch. Rational Mech. **3**, 97 (1959); E. Kröner, Arch. Rational Mech. **4**, 273 (1960); B. A. Bilby, Progr. Sol. Mech. **1**, 331 (1960).

[20] V. L. Indenbom, Certain Problems in the Physics of Plasticity, Itogi nauki (Summaries of Science) No. 3, 117 (1960).

[21] A. Love, A Treatise on the Mathematical Theory of Elasticity, Dover, N.Y., 1945.

[22] J. M. Burgers, Proc. Kon. Ned. Akad. Wet. **42**, 293, 378 (1939).

[23] V. L. Indenbom, DAN SSSR **128**, 906 (1959), Soviet Phys.-Doklady **4**, 1125 (1960).

[24] J. Blin, Acta Metallurgica **3**, 199 (1955).

[25] F. C. Frank, Proc. Phys. Soc. **A62**, 131 (1949); J. D. Eshelby, Proc. Phys. Soc. **A62**, 307 (1949); G. Leibfried and H. D. Dietze, Z. Physik **126**, 790 (1949).

[26] F. R. N. Nabarro, Phil. Mag. **42**, 1224 (1951); A. W. Saenz, J. Rational Mech. **2**, 83 (1953); R. Bullough and B. A. Bilby, Proc. Phys. Soc. **B67**, 615 (1954); A. Kosevich, JETP **42**, 152 (1962), Soviet Phys. JETP **15**, 108 (1962).

[27] J. D. Eshelby, Phys. Rev. **90**, 248 (1953); J. Weertman, Metallurg. Soc. Conf. **9**, 205 (1961).

[28] Indenbom, Nikitenko, and Milevskiĭ, DAN SSSR **141**, 1360 (1961), Soviet Phys.-Doklady **5**, 1034 (1962); FTT **4**, 231 (1962), Soviet Phys. Solid State **4**, 235 (1962).

[29] K. P. Ryaboshapka and L. V. Tikhonov, FMM **11**, 489 (1961); **12**, 3 (1961).

[30] V. L. Indenbom, Kristallografiya **2**, 594 (1957), Soviet Phys. Crystallography **2**, 587 (1958).

[31] A. N. Orlov, FTT **4**, No. 3 (1962), Soviet Phys. Solid State **4**, in press.

[32] E. Kröner and G. Rieder, Z. Physik **145**, 424 (1956).

[33] E. Holländer, Czech. J. Phys. **B10**, 409, 479, 551 (1960).

[34] A. Seeger, Dislocations and Mech. Properties of Crystals, Wiley, N. Y., 1957. Pfleiderer, Seeger, and Kröner, Z. Naturf. **15a**, 758 (1960).

[35] J. I. Frenkel and T. A. Kontorova, JETP **8**, 89, 1340, 1349 (1938).

[36] A. Foreman, Acta Metallurgica **3**, 322 (1955); A. J. E. Foreman and W. M. Lomer, Phil. Mag. **46**, 73 (1955); J. D. Eshelby, Phil. Mag. **40**, 903 (1949).

[37] Huntington, Dickey, and Thomson, Phys. Rev. **100**, 1117 (1955).

[38] V. L. Indenbom, Kristallografiya **3**, 197 (1958), Soviet Phys.-Crystallography **3**, 193 (1958).

[39] T. A. Kontorova, Nekotorye problemy prochnosti tverdogo tela (Certain Problems in the Strength of Solids), Moscow, AN SSSR 1959, p. 99.

[40] F. C. Frank and J. H. van der Merwe, Proc. Roy.

Soc. **198**, 205, 217 (1949).

[41] R. Becker, J. Phys. et radium **12**, 332 (1951).

[42] J. W. Cahn, Acta Metallurgica **8**, 554 (1960); A. L. Roĭtburd, Sb. trudov TsNIIChM (Collected Works of the Central Scientific Research Institute for Ferrous Metallurgy) No. 4, 56 (1960).

[43] Seeger, Donth, and Pfaff, Disc. Farad. Soc. **23**, 19 (1957); J. Lothe and J. P. Hirth, Phys. Rev. **115**, 543 (1959); J. Lothe, Phys. Rev. **117**, 704 (1960).

[44] A. Maradudin, J. Phys. Chem. Sol. **9**, 1 (1958); Ch. Lehmann and G. Leibfried, J. Phys. Chem. Sol. **6**, 195 (1958); B. A. Grinberg and A. N. Orlov, FMM **11**, 481 (1961).

[45] G. Leibfried, Z. Physik **127**, 344 (1950); F. R. N. Nabarro, Proc. Roy. Soc. **A209**, 279 (1951).

[46] J. D. Eshelby, Proc. Phys. Soc. **B69**, 1013 (1956).

[47] J. D. Eshelby, Proc. Roy. Soc. **A197**, 396 (1949).

[48] G. Schoeck, Phys. Rev. **102**, 1458 (1956); G. Schoeck and A. Seeger, Acta Metallurgica **7**, 469 (1959).

[49] A. Cottrell, Dislocation and Plastic Flow in Crystals, London, Oxford University Press, 1953.

[50] P. Haasen, Acta Metallurgica **5**, 598 (1957).

[51] W. G. Johnston and J. J. Gilman, J. Appl. Phys. **30**, 129 (1959).

[52] J. J. Gilman, Austral. J. Phys. **13**, 327 (1960); Progress in Ceramic Science **1**, 146 (1961); Plasticity, 2nd Symp. Naval Struct. Mech., Rhode Island, 1960, p. 43; J. J. Gilman and W. G. Johnston, J. Appl. Phys. **31**, 687 (1960).

[53] W. T. Read, Dislocations in Crystals, (Russ. Transl.) Metallurgizdat, 1958.

[54] W. G. Johnston and J. J. Gilman, J. Appl. Phys. **31**, 632 (1960).

[55] E. Orowan, Dislocations in Metals, AIME, 1954, p. 103.

[56] M. P. Usikov and L. M. Utevskiĭ, Metallovedenie i termicheskaya obrabotka metallov (Metal Research and Heat Treatment of Metals), No. 3 (1962).

[57] J. E. Bailey and P. B. Hirsch, Phil. Mag. **5**, 485 (1960).

[58] H. G. van Bueren, Physica **25**, 775 (1959).

[59] J. P. Hirth, J. Appl. Phys. **32**, 700 (1961).

[60] A. Seeger, Dislocations and Mech. Properties of Crystals (1957); Handb. Phys. **7/2**, 1 (1957).

[61] N. F. Mott, Trans. AIME **218**, 962 (1960); P. B. Hirsch and D. H. Warrington, Phil. Mag. **6**, 735 (1961).

[62] Seeger, Brenner, and Wolf, Z. Physik **155**, 247 (1959).

[63] H. Alexander, Z. Metallkunde **52**, 344 (1961).

[64] Seeger, Kronmuller, Mader, and Trauble, Phil. Mag. **6**, 639 (1961).

[65] H. G. van Bueren, Imperfections in Crystals, Amsterdam (1960).

[66] E. Kröner, Acta Metallurgica **9**, 155 (1961); I. M. Lifshitz, JETP **42**, No. 5 (1952).

[67] G. R. Irwin, J. Appl. Mech. **24**, 361 (1957); G. I. Barenblatt, PMM (Applied Mathematics and Mechanics) **23**, 706 (1959).

[68] V. L. Indenbom, FTT **3**, 2071 (1961), Soviet Phys. Solid State **3**, 1506 (1962).

[69] V. V. Panasyuk, Dopovidi AN USSR (Proceedings of the Academy of Sciences of the Ukrainian S.S.R.) No. 9, 185 (1960).

[70] Yu. M. Plishkin, FMM **9**, 178 (1960); DAN SSSR **137**, 564 (1961), Soviet Phys. Doklady **6**, 256 (1961).

[71] J. I. Frenkel, ZhTF **22**, 857 (1952).

[72] A. N. Orlov, FMM **8**, 481 (1959).

[73] Likhtman, Rebinder, and Karpenko, Vliyanie poverkhnostno-aktivnoĭ sredy na protsessy deformatsii metallov (Effect of Surface-active Medium on Metal Deformation Processes), Moscow, 1954; V. N. Rozhanskiĭ, UFN **65**, 387 (1958); V. I. Likhtman and E. D. Shchukin, UFN **66**, 213 (1958), Soviet Phys. Uspekhi **1**, 91 (1959).

[74] N. F. Mott, Engineering **165**, 16 (1948); J. J. Gilman, J. Appl. Phys. **27**, 1262 (1956); Fracture (Proc. Int. Conf., Massachusetts, 1959), 1959, p. 193.

[75] A. V. Stepanov, Physik. Z. Sowjetunion **2**, 537 (1932); Izv. AN SSSR (Division of Mechanical and Engineering Sciences), 797 (1937).

[76] J. Fisher, Acta Metallurgica **3**, 109 (1955); R. B. Green, Phys. Rev. **102**, 376 (1956).

[77] C. Zener, Fracturing of Metals (Amer. Soc. Met.), 1948, p. 3; N. F. Mott, J. Phys. Soc. Japan **10**, 650 (1955); A. Stroh, Advances Phys. **6**, 418 (1957).

[78] J. J. Gilman, Trans. AIME **212**, 783 (1958); V. N. Rozhanskiĭ, DAN SSSR **123**, 648 (1958); FTT **2**, 1082 (1960), Soviet Phys. Solid State **2**, 978 (1960).

[79] J. Friedel, Les dislocations, Paris, 1956; A. N. Stroh, Phil. Mag. **3**, 597 (1958).

[80] A. H. Cottrell, Trans. AIME **212**, 192 (1958).

[81] P. B. Price, J. Appl. phys. **32**, 1746 (1961).

[82] I. A. Oding, Izv. AN SSSR (Division of Technical Sciences), No. 3, 3 (1960).

[83] J. I. Frenkel, Acta Physicochimia USSR **3**, 633 (1935); Orlov, Plishkin, and Shepeleva, FMM **4**, 540 (1957).

[84] S. N. Zhurkov and T. P. Sanfirova, ZhTF **28**, 1719 (1958), Soviet Phys. Tech. Phys. **3**, 1586 (1959); see also P. Feltham and J. D. Meakin, Acta Metallurgica **7**, 614 (1959).

[85] B. Ya. Pines, FTT **1**, 265 (1959), Soviet Phys. Solid State **1**, 238 (1959); V. I. Vladimirov and L. É. Gurevich, ibid **2**, 1783 (1960), translation p. 1613 (1961); A. N. Orlov, ibid **3**, 500 (1961), translation p. 367 (1961).

[86] T. A. Kontorova and J. I. Frenkel, ZhTF **11**, 173 (1941).

[87] B. M. Strunin, FMM **13**, 33 (1962), DAN SSSR **125**, 790 (1959), Soviet Phys. Doklady **4**, 439 (1959); Zavodskaya laboratoriya (Plant Laboratory) **26**, 1123 (1960).

[88] S. D. Volkov, Statisticheskaya teoriya prochnosti (Statistical Theory of Strength), Mashgiz, 1960.

[89] Yu. A. Osip'yan and M. P. Usikov, DAN SSSR **143**, No. 2 (1962), Soviet Phys. Doklady, in press.

Translated by J. G. Adashko